

İSTANBUL TECHNICAL UNIVERSITY ★ INSTITUTE OF SCIENCE AND TECHNOLOGY

**INVESTIGATING OF INTERACTIONS BETWEEN STATIN-BASED
CHOLESTEROL LOWERING DRUGS WITH P-GLYCOPROTEIN
MEMBRANE PROTEIN BY MOLECULAR MODELING**

**M.Sc. Thesis by
Deniz KARASU**

Department : Advanced Technologies

Programme : Molecular Biology-Genetics and Biotechnology

JUNUARY 2011

**INVESTIGATING OF INTERACTIONS BETWEEN STATIN-BASED
CHOLESTEROL LOWERING DRUGS WITH P-GLYCOPROTEIN
MEMBRANE PROTEIN BY MOLECULAR MODELING**

**M.Sc. Thesis by
Deniz KARASU
(521071053)**

Date of submission : 20 December 2010

Date of defence examination: 28 January 2011

**Supervisor (Chairman) : Assist.Prof.Dr. Fatma Nese KÖK
Assoc.Prof.Dr. Cenk SELÇUKİ
Members of the Examining Committee : Assoc.Prof.Dr. Nurcan TÜZÜN (ITU)
Assoc.Prof.Dr. Ayten KARATAŞ (ITU)
Assist.Prof.Dr. Bülent BALTA (ITU)**

JANUARY 2011

İSTANBUL TEKNİK ÜNİVERSİTESİ ★ FEN BİLİMLERİ ENSTİTÜSÜ

**BİR MEMBRAN PROTEİNİ OLAN P-GLİKOPROTEİNİN STATİN BAZLI
KOLESTEROL DÜŞÜRÜCÜ İLAÇLARLA ETKİLEŞİMİNİN MOLEKÜLER
MODELLEME YOLUYLA İNCELENMESİ**

**YÜKSEK LİSANS TEZİ
Deniz KARASU
(521071053)**

**Tezin Enstitüye Verildiği Tarih : 20 Aralık 2010
Tezin Savunulduğu Tarih : 28 Ocak 2011**

**Tez Danışmanı : Yard. Doç. Dr.Fatma Nese KÖK (İTÜ)
Doç. Dr. Cenk SELÇUKİ (EU)
Diğer Jüri Üyeleri : Doç. Dr. Nurcan TÜZÜN (İTÜ)
Doç. Dr. Ayten KARATAŞ (İTÜ)
Yard. Doç. Dr. Bülent BALTA (İTÜ)**

OCAK 2011

FOREWORD

I would like to express my sincere gratitude to my thesis advisors Assist.Prof.Dr. Fatma Neşe K k and Assoc.Prof.Dr. Cenk Sel uki for their supervision, patience and invaluable scientific guidance. I would like to thank Assist.Prof.Dr. Fatma Neşe K k for her continuous support and encouragement throughout my master education.

I would also like to thank Assist.Prof.Dr. B lent Balta for his all supports. I have learnt many things about molecular dynamics simulation and other computational techniques from him and I would like to thank to him for not only being my teacher but also being a friend and help me to solve the encountered problems.

I would also like to thank to my research group friends for their support and encouragement. Especially I would like to thank to Sakip  nder and Fatih İnci who have been a help and motivation.

Finally, I thank to my family. You have always supported me and believed in me. I owe you much more than words can ever express.

January 2011

Deniz KARASU
Molecular Biology, M. Sc.

TABLE OF CONTENTS

	<u>Page</u>
TABLE OF CONTENTS	vii
ABBREVIATIONS	ix
LIST OF TABLES	xi
LIST OF FIGURES	xiii
LIST OF FIGURES	xiii
SUMMARY	xv
ÖZET	xvii
1. INTRODUCTION	1
1.1 P-glycoprotein.....	1
1.1.1 The ABC transporters.....	1
1.1.2 Tissue distribution.....	4
1.1.3 Physiological role.....	4
1.1.4 Multidrug resistance.....	5
1.1.5 Clinical importance of p-glycoprotein.....	6
1.1.5.1 Pgp-mediated <i>in vivo</i> drug-drug interactions.....	6
1.1.5.2 Overcoming Pgp-induced MDR in cancer therapy.....	7
1.2 Pgp Structure and Topology.....	9
1.3 Interaction of Pgp With Substrates, Modulators and Nucleotides.....	12
1.3.1 Drug binding.....	12
1.3.1.1 Substrate specificity.....	12
1.3.1.2 Nature of the drug binding site.....	14
1.3.2 Nucleotide binding and hydrolysis.....	15
1.4 Transport Mechanisms of Pgp.....	18
1.4.1 Hydrophobic vacuum cleaner and flippase models.....	18
1.4.2 Catalytic cycle.....	19
1.5 HMG-CoA Reductase Inhibitors (Statins).....	22
1.6 Role of P-glycoprotein on Statin Pharmacokinetics.....	23
1.7 Aim of The Study.....	25
2. METHODOLOGY	27
2.1 Molecular Dynamics Simulation.....	27
2.2 Theory.....	28
2.2.1 Potential energy function.....	32
2.3 Simulation Detail.....	33
2.3.1 Simulation system design.....	33
2.3.2 System preparation and simulations.....	34
2.4 Analysis Method.....	37
2.4.1 Root mean square deviation.....	37
2.4.2 Principal component analysis.....	38
3. RESULTS and DISCUSSION	41
3.1 Equilibration of Lipid Bilayer.....	41
3.2 Conformational Stability and Flexibility.....	43

3.3 Principal Component Analysis (PCA)	46
3.4 Inter-helical Hydrogen Bonds.....	49
3.5 ATP Binding.....	51
4. CONCLUSION.....	55
REFERENCES	57
CURRICULUM VITAE.....	75

ABBREVIATIONS

ABC	: ATP-Binding Cassette
ADP	: Adenosine Diphosphate
Arg	: Arginine
ATP	: Adenosine Triphosphate
AUC	: Area Under Curve
BBB	: Blood-Brain Barrier
CNS	: Central Nervous System
DMPC	: 1,2-dimyristoyl-sn-glycero-3-phosphocholine
EM	: Electron Microscope
FRET	: Forster resonance energy transfer
HID	: Imidazole ring of His bears and hydrogen atom on N _δ
HIE	: Imidazole ring of His bears an hydrogen atom on N _ε
HIP	: Imidazole ring of His bears tow hydrogen atoms on both N _δ
HMGR	: HMG-CoA reductase
HIS	: Histidine
ICL	: Intracellular Loop
Ile	: Isoleucine
Leu	: Leucine
MD	: Molecular Dynamics
Met	: Methionine
MDR	: Multidrug Resistance
NADP	: Nicotinamide adenine dinucleotide phosphate
NADPH	: Reduced form of NADP
NBD	: Nucleotide Binding Domain
NCI	: National Cancer Institute
PCA	: Principal Component Analyses
PDB	: Protein Data Bank
Pgp	: P-glycoprotein
Phe	: Phenylalanine
PME	: Particle Mesh Ewald
Pro	: Proline
RMSD	: Root Mean Square Deviation
RMSF	: Root Mean Square Fluctuation
RNA	: Ribonucleic Acid
Ser	: Serine
SNPs	: Single Nucleotide Polymorphisms
SPC	: Single point charge
Thr	: Threonine
Trp	: Tryptophan
Tyr	: Tyrosine
TMD	: Trans-Membrane Domain

LIST OF TABLES

	<u>Page</u>
Table 1.1: Chemotherapeutic Drugs and Other Compounds.....	13
Table 2.1: Summary of Simulations	34

LIST OF FIGURES

	<u>Page</u>
Figure 1.1 : Molecular architecture of ABC transporters.	3
Figure 1.2 : Structure of Pgp.	10
Figure 1.3 : Nucleotide binding domain.	16
Figure 1.4 : Statins	24
Figure 2.1 : Range of time scales for dynamics in biomolecular systems.....	27
Figure 2.2 : Examples of interaction functions in modern force fields.	29
Figure 2.3 : Simplified flowchart of a typical molecular dynamics simulation.....	31
Figure 2.4 : Simulation system: Pgp is shown in surface representation.....	34
Figure 2.5 : Docking of lactone atorvastatin.	35
Figure 2.6 : ATP docking.....	36
Figure 3.1 : Area per lipid of DMPC.....	42
Figure 3.2 : Deuterium order parameters of DMPC bilayer.	43
Figure 3.3 : RMSD of simulations.....	44
Figure 3.4 : RMSD of LACAVA simulation.	45
Figure 3.5 : RMSF of simulations.	45
Figure 3.6 : B-factor representation of LACAVA simulation.	46
Figure 3.7 : PCA of Pgp simulations	47
Figure 3.8 : Covariance matrix of simulations.	48
Figure 3.9 : LACAVA inter-helical hydrogen bonding.....	50
Figure 3.10 : Interdomain hydrogen bonding profile.	51
Figure 3.11 : Distance between Walker A and LSGGQ for APO simulation.....	52
Figure 3.12 : Distance between Walker A and LSGGQ for AFMRF simulation.	53
Figure 3.13 : Distance between Walker A and LSGGQ for LACAVA simulation.	53

INVESTIGATING OF INTERACTIONS BETWEEN STATIN-BASED CHOLESTEROL LOWERING DRUGS WITH P-GLYCOPROTEIN MEMBRANE PROTEIN BY MOLECULAR MODELING

SUMMARY

P-glycoprotein (Pgp) is a multidrug resistance protein whose function is to expel the toxic compounds out of the cell and in this way protect the cell from the harmful effect of these compounds. Pgp plays a critical role during medication since it can export different types of drugs ranging from cancer therapeutics to cardiovascular disease drugs. In order to increase the effectiveness of these drugs, there is a need to block Pgp or design drugs which can bypass Pgp during medication. To be able to do that, it is first necessary to understand mechanism of Pgp.

The aim of this study is to understand the mechanism of Pgp by using molecular dynamic simulation. To do this, ALLM (N-acetyl-lue-leu-methinonal), AFMRF (N-acetyl-phe-met-arg-phe-al) linear peptides known as Pgp substrates and atorvastatin, a cholesterol lowering drug, was used as model compounds. First, the integration of the Pgp into a lipid bilayer was done and its stability was checked. Then to supply the required energy for transportation, two MgATP were docked into the nucleotide binding pocket of Pgp. For each simulation, different substrates were docked into this system and simulated for 10 ns.

As a result of the simulations, no interaction could be detected between the linear peptides and Pgp. The reason of this situation could be the insufficient number of peptide per transport cycle used during simulations. Pgp can export more than one molecule per transport cycle and need to fill its pocket with enough molecules to function. Lactone form of atorvastatin, on the other hand, was found to interact with Pgp as expected and led to an asymmetrical closure of nucleotide binding domains during 10 ns simulation.

BİR MEMBRAN PROTEİNİ OLAN P-GLİKOPROTEİNİN STATİN BAZLI KOLESTEROL DÜŞÜRÜCÜ İLAÇLARLA ETKİLEŞİMİNİN MOLEKÜLER MODELLEME YOLUYLA İNCELENMESİ

ÖZET

P-glikoprotein (Pgp), bir çoklu-ilaç direnç proteini olup fonksiyonu toksik maddeleri hücreden uzaklaştırma yolu ile hücreyi bu maddelerin zararlı etkilerin korumaktır. Pgp, kanser terapiden kalp damar hastalıklarına kadar çeşitli tipte ilacı uzaklaştırabildiği için tedavi sürecinde kritik rol oynar. Bu ilaçların etkisini artırabilmek için Pgp'nin çalışmasını durduracak yada Pgp'ye uğramadan hücreye ulaşabilecek ilaçların tasarlanmasına ihtiyaç vardır. Bunu başarabilmek için ilk olarak Pgp'nin mekanizmasını anlamak gerekmektedir.

Bu çalışmanın amacı moleküler dinamik simülasyon kullanarak Pgp'nin mekanizmasını anlamaktır. Bunun için Pgp substratı olduğu bilinen ALLM (N-asetil-leu-leu-met-al), AFMRF (N-asetil-phe-met-arg-phe-al) doğrusal peptidleri ve kolesterol düşürücü atorvastatin'nin lakton formu örnek molekül olarak kullanıldı. İlk olarak Pgp'nin lipid zar içine yerleştirilmesi gerçekleştirildi ve stabilitesi gözden geçirildi. Arkasından Pgp nin taşıma için gerekli enerjiyi tedarigine yönelik proteinin ilgili nükleotid bağlanma bölgelerine iki adet MgATP molekülü yerleştirildi. Her bir simülasyon için oluşturulan bu yapıya farklı substratlar yerleştirildi ve 10 ns boyunca simüle edildi.

Çalışma neticesinde doğrusal peptid zincirlerinin pek Pgp ile etkileşmediği gözlemlendi. Bunun sebebi peptid büyüklüklerinin yetersiz kalması olabilir. Çünkü Pgp aynı anda birden fazla ilacı taşıyabilme kapasitesine sahip bir proteindir. Bu peptidler için de birden fazlası taşıma için gerekli olabilir. Ancak diğer taraftan atorvastatin lakton formu Pgp ile beklenen şekilde etkileşime girdi ve 10 ns simülasyon boyunca nükleotid bağlanma domainlerinde asimetric bir kapanmaya neden oldu.

1. INTRODUCTION

1.1 P-glycoprotein

1.1.1 The ABC transporters

P-glycoprotein (Pgp) is a 170 kDa member of the ATP-Binding cassette (ABC) transporters superfamily that was first identified in drug-resistant Chinese hamster ovary cells by its ability to reduce the rate of drug uptake. Cell lines that were initially selected for resistance to one cytotoxic drug were later shown to display cross-resistance to other structurally unrelated cytotoxic compounds [1-3]. In nearly all cases, the drug-resistant cell lines showed over-expression of a 170 kDa glycosylated plasma membrane protein when compared to the drug-sensitive parent cell lines [4,5]. The protein was termed P-glycoprotein (Pgp) because it appeared to affect the permeability of the membrane to cytotoxic compounds [6].

In 1986, three groups reported the cloning and sequencing of the gene responsible for Pgp-mediated drug resistance from hamster [7], human [8] and mouse [9] cell lines. It is a product of the MDR1 (ABCB1) gene in humans and has two homologues in mice (*abcb1a* and *abcb1b*). It was subsequently shown that Pgp is an ATP-dependent drug pump that can transport a broad range of structurally unrelated compounds out of the cell [10].

ATP-binding cassette transporters (ABC-transporter) are members of a protein superfamily that is one of the largest and most ancient families with representatives in all extant phyla from prokaryotes to humans [11]. ABC transporters are transmembrane proteins that utilize the energy of adenosine triphosphate (ATP) hydrolysis to carry out certain biological processes including translocation of various substrates across membranes [12,13] and non-transport-related processes such as translation of RNA and DNA repair [14]. They transport a wide variety of substrates across extra- and intracellular membranes, including metabolic products, lipids and sterols, and drugs. Proteins are classified as ABC transporters based on the sequence and organization of their ATP-binding cassette (ABC) domain(s). ABC transporters

are involved in tumour resistance, cystic fibrosis, bacterial multidrug resistance, and a range of other inherited human diseases.

Cellular survival requires the generation and maintenance of electrical and chemical concentration gradients across the generally impermeable cell membrane. ATP-binding cassette (ABC) transporters are key participants in this process, and typically use the favourable chemical energy of ATP hydrolysis to translocate molecules across membranes in a thermodynamically unfavourable direction. ABC transporters function as either importers, which bring nutrients and other molecules into cells, or as exporters, which pump toxins, drugs and lipids across membranes.

Members of the ABC transporter family are present in organisms from all kingdoms of life; whereas exporters are found in both eukaryotes and prokaryotes, importers seem to be present exclusively in prokaryotic organisms. ABC transporters constitute the largest protein family in *E. coli*, including 80 distinct systems that represent 5% of the genome [18], whereas 50 ABC transporters are present in humans [19] and seventeen of these proteins are source of some diseases [20].

ABC transporters have a characteristic architecture that consists minimally of four domains Figure 1.1: two transmembrane domains (TMDs) that are embedded in the membrane bilayer, and two ABCs (or nucleotide-binding domains (NBDs)) that are located in the cytoplasm. At the sequence level, the superfamily of ABC transporters is identified by a characteristic set of highly conserved motifs that are present in the ABCs. By contrast, the sequences and architectures of the TMDs are variable, reflecting the chemical diversity of the translocated substrates. Beyond these four domains, additional elements can fuse to the TMDs and/or ABCs of ABC transporters and probably have regulatory functions [21]. For prokaryotic ABC transporters that function as importers, substrate translocation is also dependent on another protein component, a high-affinity binding protein that specifically associates with the ligand in the periplasm for delivery to the appropriate ABC transporter [22]. In ABC importers, the TMDs and NBDs are separate polypeptide chains. In bacterial exporters, by contrast, a TMD is fused to a NBD, generating a 'halftransporter' that forms a homodimer or heterodimer to generate the functional unit. Many eukaryotic ABC exporters are expressed with all four domains in a single polypeptide chain [23].

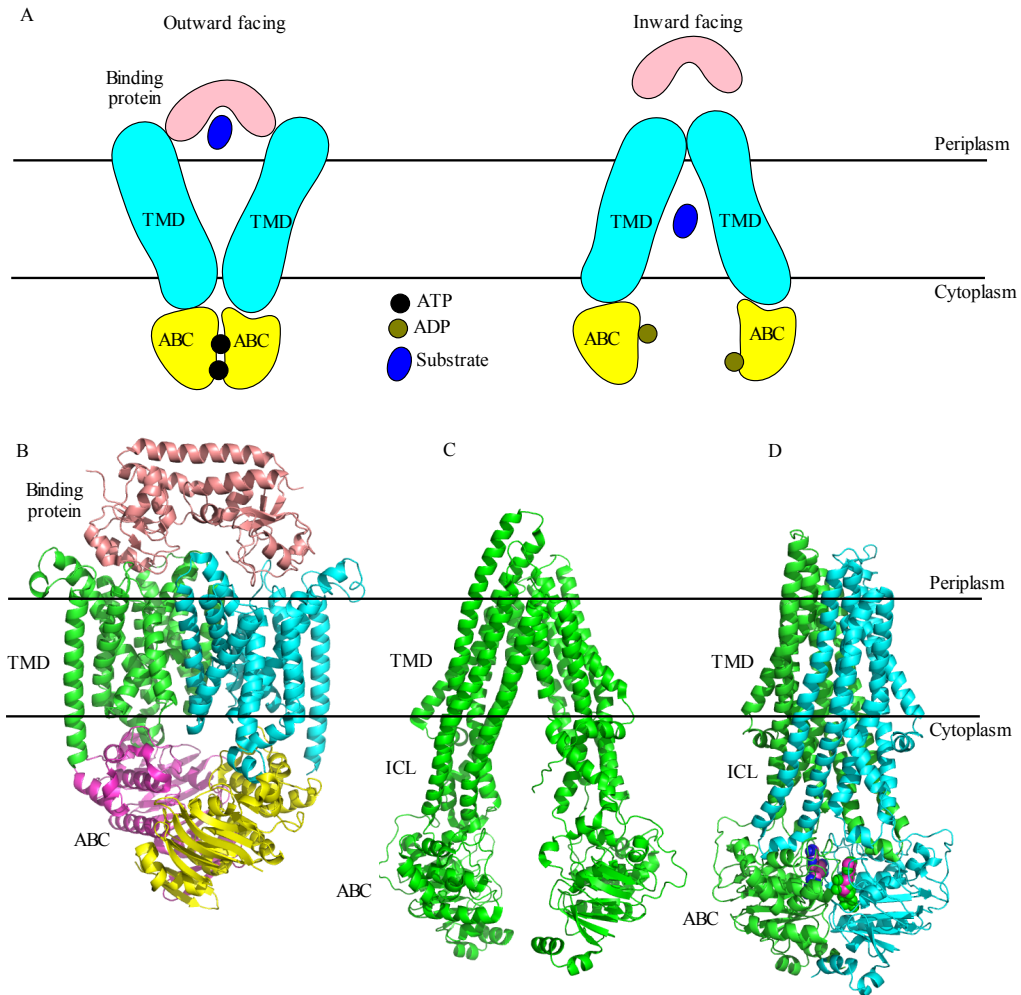


Figure 1.1 : Molecular architecture of ABC transporters. **A)** A cartoon of the modular organization of ATP-binding cassette (ABC) transporters, which are composed of two transmembrane domains (TMDs) and two ABC domains (or nucleotide-binding domains). The binding protein component that is required by importers is also shown. Two conformational states of the ABC transporter-outward facing and inward facing, with the substrate-binding site orientated towards the periplasmic (extracellular) and cytoplasmic (intracellular) regions, respectively - are depicted to show the alternating access mechanism of transport. **B)** The *E. coli* vitamin B12 importer BtuCDF[15] (PDB 2QI9). The core transporter consists of four subunits: the two TMD BtuC subunits (green and blue) and the two ABC BtuD subunits (yellow and magenta). This complex also contains one copy of BtuF, the periplasmic binding protein (pink). **C)** The mouse p-glycoprotein multidrug exporter [16] (PDB 3G60). P-glycoprotein is a monomer and all four domain is combined into a single polypeptide chain. **D)** The *Staphylococcus aureus* Sav1866 multidrug exporter [17] (PDB code 2HYD). Sav1866 consists of two subunits (green and blue), which contain a fused TMD and ABC domain. The nucleotides that are bound in this structure are shown by space-filling models. ICL, intracellular loop.

1.1.2 Tissue distribution

Early studies of Pgp distribution in human [24] and rodent [25] tissues showed that the protein is expressed at low levels in most tissues but is found in much higher amounts at the apical surface of epithelial cells lining the colon, small intestine, pancreatic ductules, bile ductules and kidney proximal tubules, and the adrenal gland. Thus, epithelial cells with excretory roles generally express Pgp. The transporter is also located in the endothelial cells of the blood–brain barrier [26], the blood–testis barrier [27], and the blood–mammary tissue barrier [28], and has recently been found to play a role in the blood–inner ear barrier, where it is expressed in the capillary endothelial cells of the cochlea and vestibule [29]. Thus the role of Pgp in the blood–brain and blood–tissue barriers is likely to protect these organs from toxic compounds that gain entry into the circulatory system. Pgp is expressed at high levels at the luminal surface of secretory epithelial cells in the pregnant endometrium [30], as well as the placenta [31], where it may provide protection for the fetus [32]. The protein is also found on the surface of hematopoietic cells, where its function remains enigmatic. The ABCB4 protein is expressed at high levels on the bile canalicular membrane of hepatocytes, in accordance with its proposed role in transport of PC into the bile [33].

1.1.3 Physiological role

The tissue localization of Pgp suggests that the protein plays a physiological role in the protection of susceptible organs such as the brain, testis, and inner ear from toxic xenobiotics, the secretion of metabolites and xenobiotics into bile, urine, and the lumen of the gastrointestinal tract, and possibly the transport of hormones from the adrenal gland and the uterine epithelium. These ideas have been strongly supported by studies on transgenic knockout mice lacking one or both of the genes encoding the drug-transporting Pgps *Abcb1a* and *Abcb1b*. Both single- and double-knockout mice are fertile, viable, and phenotypically indistinguishable from wild-type mice under normal conditions. So Pgp does not appear to fulfill any essential physiological functions. However, Pgp knockout mice showed radical changes in the way that they handled a challenge with many drugs [34]. *mdr3* knockout mice displayed a disrupted blood–brain barrier and were 100-fold more sensitive to the pesticide

ivermectin, which was neurotoxic to the animals [35]. This Pgp isoform appears to play the major role in preventing accumulation of drugs in the brain [34,36]. The double-knockout mouse has proved useful in evaluating the effect of Pgp-mediated transport on drugs that are targeted to the central nervous system [37]. Certain dogs of the collie lineage [38] and several other dog breeds [39,40] have a naturally occurring lack of Pgp due to a frameshift mutation in the MDR1 gene and are also hypersensitive to ivermectin. To date, no human null alleles have been reported, despite widespread use of drugs that are Pgp substrates.

Pgp in the intestinal epithelium plays an important role in the extrusion of many drugs from the blood into the intestinal lumen, and in preventing drugs in the intestinal lumen from entering the bloodstream. Pgp activity can therefore reduce the absorption and oral bioavailability of those drugs that are transport substrates. Due to the prevalence of Pgp in a variety of barrier tissues, and the physiological role that it plays in the bioavailability and pharmacokinetics of clinically administered drugs, the interaction of drugs with Pgp is an important factor that needs to be considered when designing a treatment regimen.

1.1.4 Multidrug resistance

The overexpression of Pgp is one of the main causes of cancer cells becoming simultaneously resistant to multiple chemotherapeutic drugs, resulting in a condition known as multidrug resistance (MDR) [41]. The development of MDR is a major obstacle to treating cancer, and Pgp is thought to contribute to chemotherapy drug resistance in 50% of human cancers [10]. Some tumours are inherently drug-resistant, whereas others develop MDR over the course of treatment. Cancers of the colon, liver, pancreas and kidney tend to be intrinsically drug-resistant, whereas leukemias, myeloma, ovarian and breast cancers tend to develop MDR as a result of chemotherapeutic intervention. Cancers that acquire MDR due to overexpression of Pgp after chemotherapy show a greater response to Pgp inhibitors than cancers expressing elevated levels of Pgp at the time of diagnosis, likely because other mechanisms of resistance are present in the latter [42]. The ability of Pgp to confer drug resistance *in vivo* has been demonstrated with the retroviral transfer of MDR1 into murine bone marrow cells, resulting in resistance to the cytotoxic drug taxol [43]. Using positron emission tomography and n C-labelled verapamil as a substrate,

cyclosporin A was shown to inhibit the human BBB Pgp [44]. This method is useful for monitoring the *in vivo* activity of Pgp.

Since Pgp causes *in vivo* drug resistance, inhibition of Pgp-mediated drug efflux has been proposed as one way to increase the uptake of chemotherapy drugs into MDR tumour cells. Pgp modulators, which are MDR reversal agents, block the drug efflux ability of Pgp by interacting at either the substrate binding pocket [45], or one of several proposed allosteric binding sites [46]. Pgp modulators alone are not toxic to MDR cells, but a combination of modulator and chemotherapy drug is highly cytotoxic. Pgp modulators belong to many different structural classes, and some are thought to act as alternative substrates for Pgp, engaging the protein in a futile cycle of ATP hydrolysis and transport. Clinical trials involving the Pgp modulator cyclosporin A have shown that acute myeloid leukemia patients who were treated with the modulator, as well as cytarabine and daunorubicin, had increased survival over patients treated with only standard chemotherapy drugs [47]. However, the use of modulators in cancer treatment has not generally been very successful [48]. Due to the variety of human tissues in which Pgp is normally found, the use of modulators can cause toxicity problems and needs to be carefully monitored. The toxicity and limited efficacy of Pgp modulators *in vivo* has hindered their use in the treatment of MDR cancers, and highlights the need for a greater understanding of the transporter.

1.1.5 Clinical importance of p-glycoprotein

1.1.5.1 Pgp-mediated *in vivo* drug-drug interactions

A main focus of Pgp research thus far has been to reverse the Pgp-induced MDR phenotype in tumour cells, but with hundreds of potential substrates, there are numerous other clinical implications of Pgp expression. Pgp transports a wide variety of drugs used in the treatment of human diseases including anti-cancer drugs, antibiotics, HIV protease inhibitors, tyrosine kinase inhibitors, calcium channel blockers and cardiac glycosides. Simultaneously treating patients with different drugs is common practice, and with the ability of Pgp to affect the absorption, distribution and bioavailability of drugs, co-administration of multiple drugs that are Pgp substrates could have serious side effects [49]. The *in vivo* interaction of multiple drugs with Pgp can also be beneficial. Studies on Pgp knockout mice showed up to a 100-fold increase in central nervous system (CNS) penetration of

drugs [50], indicating that Pgp modulators could be used to enhance the treatment of neurological disorders by increasing drug access to the brain.

Numerous adverse reactions have been observed in the clinic as a result of simultaneously treating patients with multiple Pgp substrates. Administration of the calcium channel blocker, mibefradil, and the immune suppressor, tacrolimus, to a liver transplant patient resulted in unexpected cognitive side effects, because both drugs interact with cytochrome P450 and are Pgp modulators [51]. Decreased metabolism of tacrolimus resulted in elevated blood levels that overwhelmed Pgp, and the drug passed through the BBB, causing CNS toxicity. Pgp expression in the brush-border of the small intestine normally prevents the absorption of numerous orally administered drugs. Administering rifampin with digoxin concomitantly resulted in a significant decrease in digoxin absorption, due to a 3.5 fold increase in Pgp expression caused by rifampin [52]. An increase in Pgp expression has also been observed after administration of St. John's wort [53], which is commonly found in over-the-counter herbal medications, demonstrating the potential for serious side effects if patients take herbal remedies in conjunction with drugs prescribed by their doctor. Due to the potential negative side effects of multiple drugs interacting simultaneously with Pgp, many compounds are now screened for Pgp transport ability during the drug discovery process. Drugs can be screened using *in vitro* and *in vivo* assays, as well as with computational methods based on *in silico* models of Pgp quantitative structure-activity relationships (QSAR) [54].

1.1.5.2 Overcoming Pgp-induced MDR in cancer therapy

The overexpression of Pgp in tumour cells is one of the main causes of MDR, which is responsible for drug resistance in 50% of human cancers [41]. There was initial optimism that the use of Pgp reversal agents would allow oncologists to overcome the Pgp-induced drug resistance in MDR tumours. Although there has been some success using Pgp modulators to treat juvenile cancers, their use in clinical trials of adult cancers has been disappointing. The lack of efficacy of Pgp modulators in early clinical trials discouraged many pharmaceutical companies from further pursuing Pgp inhibition as a method of treating MDR [55]. A critical analysis of these studies indicates that their results may not be very reliable [45], and reveals a number of reasons why they failed to show a beneficial effect. One of the main problems was the lack of a consistent diagnosis of the MDR phenotype, resulting in the inclusion of

patients in the clinical trial who did not have drug resistance as a result of Pgp overexpression.

First generation modulators (cyclosporin A, verapamil) were often pharmacologically active, and had low efficacy and high toxicity at clinically relevant doses, although some trials did show promising results [46]. Second generation modulators (PSC833 (valsopodar)) were more efficacious at low doses and had no inherent toxicity, but many were substrates of cytochrome P450 3A. This resulted in adverse pharmacokinetic interactions, and increased toxicity *in vivo* when the treatment drug was also a P450 3A substrate. Problems with first and second generation modulators led to the careful design of third generation modulators (LY335979 (zosuquidar), GG918 (elacridar)) with low pharmacokinetic interactions and high affinity for Pgp. Currently, Phase I, II and III clinical trials involving third generation Pgp modulators are still under way. The results of well-designed Phase III clinical trials involving third generation modulators will be vital in determining if inhibition of Pgp can result in increased patient survival [55].

As an alternative to reversing MDR by suppressing Pgp function, it may be possible to exploit Pgp activity to induce cytotoxicity in MDR tumour cells. A thiosemicarbazone derivative (NSC73306) was identified in an NCI drug screen that looked for the potential interaction of candidate anti-cancer drugs with the 48 known human ABC proteins in the NCI-60 cell lines [56]. Surprisingly, compounds were identified whose activity increased rather than decreased in the presence of ABCB1. NSC73306 appears to interact with Pgp through an allosteric mechanism, and is cytotoxic to cells that overexpress Pgp either intrinsically, or through an acquired mechanism [57]. Administration of NSC73306 resensitized Pgp-expressing MDR carcinoma cells to other chemotherapeutic drugs, thus reversing the MDR phenotype. By selectively targeting MDR tumour cells that overexpress Pgp, NSC73306 represents a novel way of reversing Pgp-mediated MDR, and may have an important clinical impact in cancer therapy [57].

The modulation of Pgp activity is an important step in the treatment of MDR cancers, but Pgp is not the only multidrug-binding ABC protein that contributes to *in vivo* drug resistance. The second generation Pgp modulator VX-710 (biricodar) has been shown to also inhibit the function of the multidrug transporters MRP1 (ABCC1) and BCRP (ABCG2), suggesting that it may be possible to develop agents with low

toxicity and high potency against all three proteins. To evaluate the *in vivo* effects of modulators, the radiopharmaceutical Tc-99m sestamibi, which is a Pgp substrate, has been used as an imaging agent. Tc-99m sestamibi allows clinicians to evaluate the efficacy of a modulator by monitoring changes in the *in vivo* uptake of a Pgp substrate. Despite early setbacks in the development and use of Pgp modulators, the importance of MDR in limiting the successful treatment of cancer demonstrates the need for continued research into ways of overcoming it.

The use of modulators in combination with chemotherapy drugs has given promising results *in vitro*, but treatment success *in vivo* has been more difficult to obtain. The lack of success in clinical trials of Pgp modulators may be due to poor study design that did not account for Pgp single nucleotide polymorphisms (SNPs). More than 50 SNPs (and insertion/deletion mutations) have been reported for ABCB1 [58], and recent studies have shown that a silent mutation in Pgp can result in changes in the binding affinity of substrates, likely by altering the kinetics of protein folding [59]

1.2 Pgp Structure and Topology

The human Pgp (product of the MDR1 gene; ABCB1) has 1280 amino acids that are arranged as two homologous halves joined by a linker region. Each half begins with a transmembrane domain (TMD) containing six transmembrane (TM) segments followed by a hydrophilic region containing a nucleotide-binding domain (NBD or ABC) (see Figure 1.2) [8,60,61]. The presence of four domains and conserved sequences in the NBDs are characteristic of the ATP-binding cassette (ABC) family of transporters [62]. The proposed topology of Pgp (Figure 1.2A) was first confirmed through the use of Cys mutagenesis [61] and epitope insertion with immunofluorescence.

Several low-to-medium resolution electron microscopic images have been reported for Pgp, [63-66] the best of which is a ~ 8 Å cryo-electron microscopy structure with bound AMP-PNP [66]. The ~ 8 Å structure is important because it give us some opinion about nucleotide bound state of p-glycoprotein. This nucleotide bonded Pgp is very similar with Sav1866 (see 1.1D) [67] bound to ADP structure. This structure confirms the presence of two closely associated NBDs and TMDs consisting of 12 helices in total, which reorient upon ATP binding. But cross-linking experiments have shown that TM helix 6 is close to TM10, 11, and 12, and that TM helix 12 is

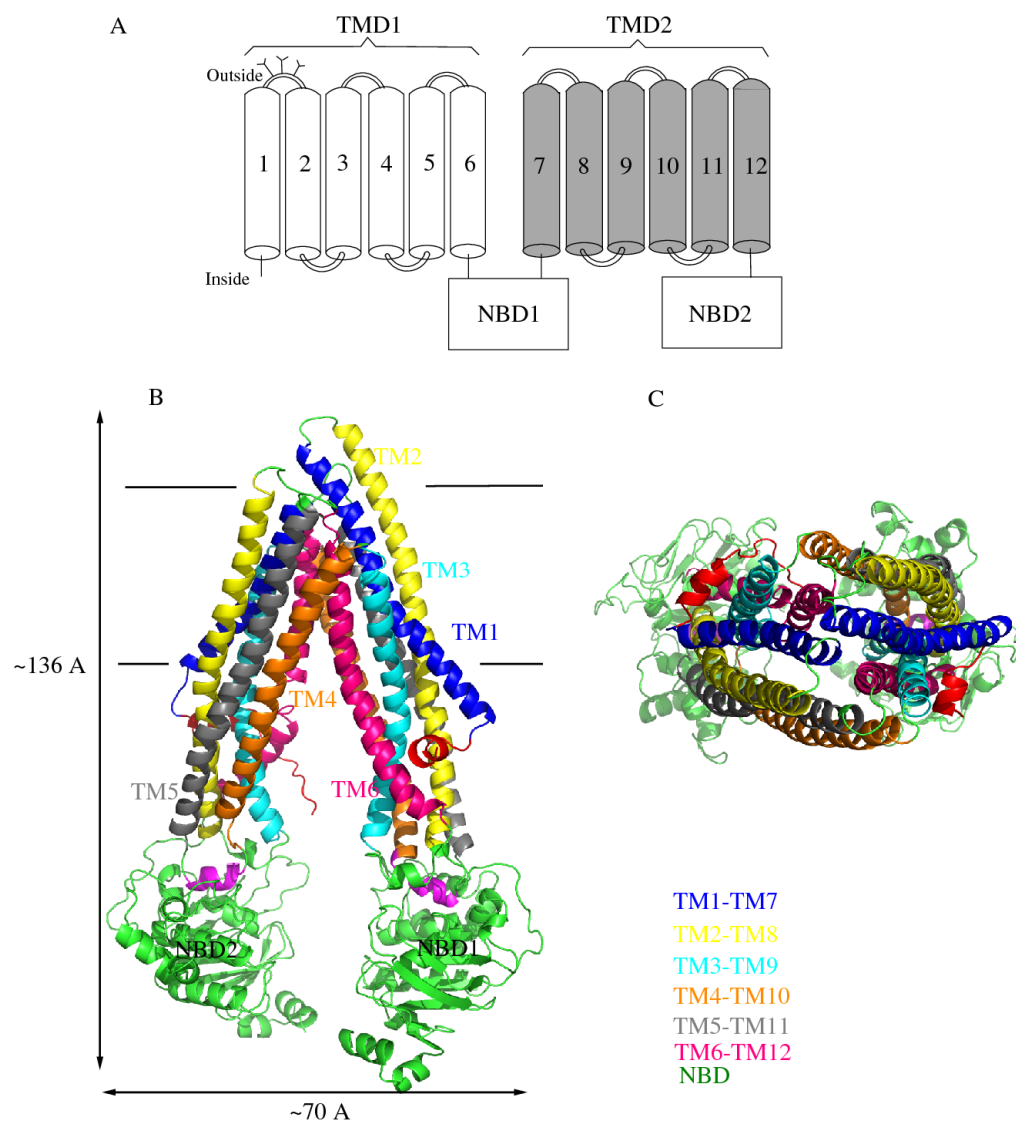


Figure 1.2 : Structure of Pgp: A) The white cylinders represent the TM segments in TMD1, while the grey cylinders represent TM segments within TMD2. The branched lines represent the glycosylation sites and the rectangles represent the NBDs. B) Cartoon representation p-glycoprotein (pdb 3G60). Symmetrical α -helices represented by similar color. C) View of the NBDs shown from the cytosol looking up toward the membrane.

close to TM4, 5, and 6 [68]. From Cys mutagenesis studies, the drug-binding sites of Pgp appear to reside in the membrane-embedded region, at the interface between the two halves of the protein, in TM helices 4–6 and 9–12 [69-73]. Fluorescence studies have confirmed that the NBDs of Pgp are closely associated [74] and lie close to the membrane surface,[75] and showed that the drug-binding sites reside in the region of

the protein located in the inner leaflet of the membrane [76,77]. A recent study used cysteine mutagenesis and chemical cross-linking to show that Pgp shares important features of its domain architecture with Sav1866; in particular, the long intracellular loops of one TMD appeared to contact the opposing NBD, a feature not observed in bacterial ABC importers [78].

An important development in our understanding of mammalian ABC drug pumps was the recent publication of the 3.8 Å crystal structure of mouse Pgp in the absence of nucleotide [16] (Figure 1.2 B and C). The most remarkable feature of this “apo” structure is how well it agrees with both the bacterial ABC protein structures and the biochemical/biophysical data generated on Pgp structure and function over the past 30 years [79]. The structure of Pgp (Figure 1.2) represents a nucleotide-free inward-facing conformation arranged as two “halves” with pseudo two-fold molecular symmetry spanning ~136 Å perpendicular to and ~70 Å in the plane of the bilayer. The nucleotide-binding domains (NBDs) are separated by ~30 Å. The inward-facing conformation, formed from two bundles of six transmembrane helices (TMs 1 to 3, 6, 10, 11 and TMs 4, 5, 7 to 9, 12), results in a large internal cavity open to both the cytoplasm and the inner leaflet [16]. This crossover is very reminiscent of the Sav1866 (Figure 1.1 D) and corrected MsbA structures [80]. The Pgp structure was solved in the absence of nucleotide, and the two NBDs are located ~30 Å apart (Figure 1.2 A). The open-apo structure of MsbA from *E. coli* displays a much wider separation of the NBD domains. In contrast, one apo structure and the nucleotide-bound MsbA structures, as well as the structures of Sav1866 (both nucleotide-bound [17,67]) and other bacterial ABC proteins, [23,81] show a tight association of the NBDs. The arrangement of the NBDs is already controversial, since some evidence supports the wide apo-MsbA structure [82-84]. It remains unclear whether such an open structure exists for native MsbA, since it would require a dramatic conformational change to close the NBDs upon nucleotide binding/hydrolysis. While the NBD separation is only 30 Å in the Pgp structure, versus ~50 Å in MsbA, Aller et al. suggest that Pgp may open even wider to accommodate very large substrates [16]. Further work will be required to distinguish whether this open conformation is a real feature of native Pgp or a crystal-packing artifact.

The crystal structure of Pgp has some missing residues [16]. The N-terminus (residues 1-33) was not visualized and no electron density was present for most of

the linker region (residues 627-683), which is likely a flexible region connecting the two halves of Pgp [85]. Interestingly, both full-length Pgp and co-expressed half-molecules of Pgp devoid of the linker region (Δ 627-683) share similar drug-stimulated ATPase activity suggesting that an intact linker is not required for drug-coupled ATPase hydrolysis [86].

1.3 Interaction of Pgp With Substrates, Modulators and Nucleotides

1.3.1 Drug binding

1.3.1.1 Substrate specificity

Pgp shows broad substrate specificity, recognizing hundreds of compounds as small as 330 daltons up to 4000 daltons [87,88]. In general, Pgp substrates tend to be large, hydrophobic, amphipathic molecules with aromatic rings and a positively-charged nitrogen atom [10-89], but these are not absolute requirements. However, it is difficult to make generalizations about the properties of compounds that interact with Pgp, and many substrates have been identified that do not strictly conform to these descriptors. For example, a variety of linear and cyclic peptides and ionophores are known to interact with the protein [90-92], yet peptides are smaller than typical substrates and often lack aromatic rings. Pgp substrates include classical chemotherapeutic drugs (such as anthracyclines, Vinca alkaloids, and taxols), new classes of anticancer agents such as tyrosine kinase inhibitors, human immunodeficiency virus (HIV) protease inhibitors, immunosuppressants, ionophores, peptides, fluorescent dyes, steroids, cardiac glycosides, and many others (see Table 1.1) [79]. There is a variation in the binding affinity (K_d of Pgp for drugs that covers 4 orders of magnitude [17], indicating that the protein is able to distinguish between different substrates.

Substrates are thought to interact with Pgp via hydrogen bonding, as well as hydrophobic and van der Waal's interactions, in a large, flexible, substrate binding pocket. Based on FRET mapping studies, the binding pocket is thought to be located in the cytoplasmic leaflet of the TM region of the protein [76,77]. It has been proposed that drugs bind to Pgp by an induced-fit type of mechanism [93], in which substrates enter the substrate binding pocket and create their own specific drug binding site using residues from a number of different TM helices. This mechanism

Table 1.1: Chemotherapeutic Drugs and Other Compounds That Interact with p-glycoproteins [79].

Group	Compound
analgesics	morphine
antiarrhythmics	amiodarone, propafenone, quinidine
antibiotics	erythromycin, gramicidinD
anthracenes	bisantrene, mitoxantrone
anthracyclines	doxorubicin, daunorubicin
camptothecins	topotecan
epipodophyllotoxins	etoposide, teniposide
taxanes	paclitaxel, docetaxel
Vincaalkaloids	vinblastine, vincristine
antiemetics	ondansetron
antiepileptics	felbamate, topiramate
antihelminthics	ivermectin
antihistamines	fexofenadine, terfenadine
antihypertensives	reserpine, propranolol
antiviral drugs	nelfinavir, ritonavir, saquinavir
calcium-channel blockers	azidopine, diltiazem, nifedipine, verapamil
calmodulin antagonists	chlorpromazine, trans-flupentixol
cardiac glycosides	digoxin
fluorescent dyes	calcein-AM, Hoechst 33342, rhodamine 123, tetramethylrosamine
H ₂ -receptor antagonists	cimetidine
HMG-CoA reductase inhibitors	lovastatin, simvastatin, atorvastatin
immunosuppressive agents	cyclosporinA, tacrolimus (FK506)
natural products	colchicine, curcuminoids
pesticides	N-acetyl-LLY-amide (ALLN), leupeptin, pepstatinA, valinomycin
pesticides	cypermethrin, endosulfan, fenvalerate, methylparathion
steroids	aldosterone, corticosterone, cortisol, dexamethasone
tyrosine kinase inhibitors	gefitinib, imatinib mesylate
antialcoholism drugs	disulfiram

explains how mutations at specific residues alter the binding affinity of Pgp for one substrate, but have no effect on the affinity for other substrates [94].

There have been attempts to associate the “affinity” of a Pgp substrate or modulator with its physical, chemical or structural properties through the use of QSARs. The search for specific structural characteristics common to all Pgp substrates has met with limited success. There is no common “pharmacophore” that can be used to identify a particular drug as a Pgp substrate [79]. The best general description of a

Pgp substrate is that it contains 2 or 3 electron donor (hydrogen bond acceptor) groups with a fixed spatial separation [95,96]. Seelig and co-workers examined over 100 compounds known to interact with Pgp and classified them based on the number and separation distance of electron donor groups. All substrates examined were found to possess either 2 or 3 electron donor groups separated by 2.5 or 4.6 Å. Other researchers subsequently suggested combinations of electron donors, hydrophobic groups, and/or aromatic rings in specific spatial organizations [97-99]. A more recent 3-dimensional approach suggested that molecules with two H-bond acceptors 11.5 Å apart and two H-bond donors 16.5 Å apart would be Pgp substrates [100]. TM regions of Pgp thought to be involved in drug binding contain a large proportion of amino acid side chains that can act as hydrogen bond donors, facilitating interaction with substrate electron donor groups [95]. The fluorescence properties of aromatic Trp residues in Pgp are sensitive to substrate binding [101], and may be involved in stacking interactions between drug substrates and aromatic side chains in the Pgp drug binding pocket [102].

1.3.1.2 Nature of the drug binding site

Pgp appears to have a large flexible binding region that can accommodate a wide range of compounds, rather than one or more well-defined binding sites. Two “functional” binding sites have been identified based on the transport of the drug substrates rhodamine 123 (R-site) and Hoechst 33342 (H-site) [103]. Two drugs that bind to the same site (either the H-site or the R-site) are proposed to show mutual inhibition of transport, whereas drugs that bind to different sites are proposed to exhibit mutual stimulation of transport. Using FRET, the locations of the H-site [76] and the R-site [77] have been mapped, and both are found within the cytoplasmic leaflet of the membrane. Analysis of the fluorescence characteristics of drugs bound to the H and R binding sites has shown that they are very hydrophobic in nature, with a polarity lower than chloroform [93], making it unlikely that the binding pocket is open to an aqueous chamber as previously suggested [64,104]. Crosslinking studies involving the insertion of Cys residues into Cys-less Pgp suggested that the substrate binding pocket is formed at the interface between the two TMDs, and involves TM helices 4, 5, and 6 in the N-terminal half of Pgp, and TM helices 9, 10, 11 and 12 in the C-terminal half [72]. The Pgp drug binding pocket is thought to be funnel-

shaped, based on both cross-linking and EM studies [16], and appears to be narrower on the cytoplasmic side where TM2-TM11 and TM5-TM8 come together [105].

Using 3-D models of Pgp substrates, Garrigues and coworkers identified two different, overlapping pharmacophores in the protein [106], which may correspond to the H and R functional binding sites. This study suggested that it was possible for either two smaller substrates to bind to Pgp at the same time, or one larger substrate to occupy both pharmacophores. A recent homology model of Pgp in the post-hydrolysis state, based on Sav1866 [107], identified three main drug binding regions; one at the cytosolic interface of the membrane, and two located within the TM helices of the TMDs. In addition, a large central binding pocket was identified that contained residues from all three regions, which is thought to represent a low affinity “escaping” site from which substrates are released [107]. In the absence of high resolution structural data for Pgp with bound substrates, homology models can give insight into the specific molecular interactions that might take place in the drug binding pocket

1.3.2 Nucleotide binding and hydrolysis

The NBDs of ABC transporters are divided into two domains, the catalytic domain and the helical domain, which are connected via the Q-loop and the Pro-loop [108]. The catalytic domain contains the Walker A and B motifs, as well as the H-loop and D-loop, while the helical domain contains the ABC signature C motif. The binding of ATP to ABC proteins requires the Walker A and B motif of one NBD, along with the C motif of the partner NBD (see Figure 1.3). Thus, two ATP molecules are bound to each ABC protein, at the interface between the NBDs. The C motif interacts specifically with the γ -phosphate moiety of ATP, allowing for stable dimerization of the NBDs when ATP is bound, but not when ADP is present. Close association of the NBDs in the absence of nucleotide would facilitate dimer formation upon ATP binding, and has been seen in the crystal structures of several ABC proteins [15, 80, 109]. Cryo-EM [64,66,110] and biochemical studies of Pgp [74,111] have also suggested close association of the NBDs.

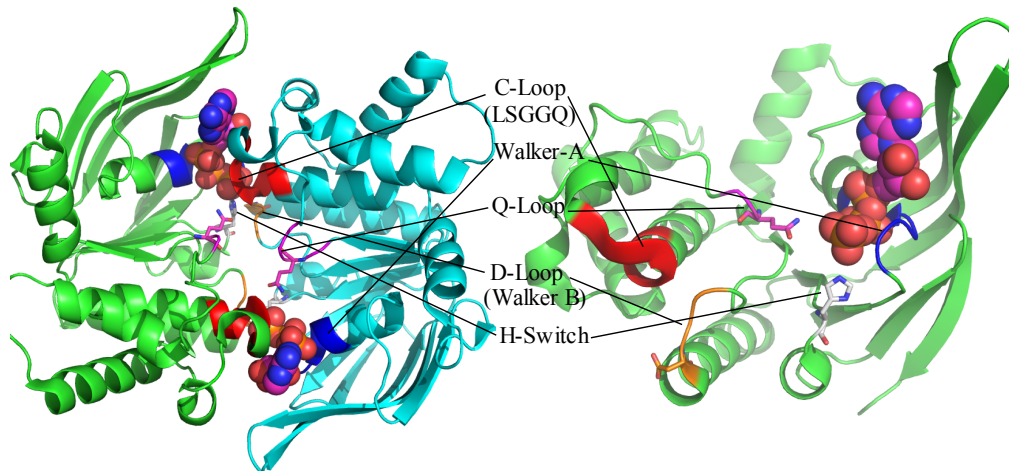


Figure 1.3 : Nucleotide binding domain: The X-ray crystal structure of the NBDs of the bacterial MJ0796 ABC ATPase dimer (1L2T.pdb) with bound nucleotide. The conservative motifs (Walker A, B, C-Loop, D-Loop, H-Switch) are showed on cartoon representation.

Mutational analysis of the NBDs has identified a number of key residues that are involved in nucleotide binding and hydrolysis. The crystal structure of the catalytically inactive E171Q mutant of the NBD subunit MJ0796 first showed the formation of a nucleotide sandwich dimer through the stable binding of two ATP molecules [112]. A similar structure was observed for the NBDs of HlyB [113]. Corresponding mutations of Glu residues in mouse *abcb1a* Pgp (E552A/E1197A) resulted in tight occlusion of bound nucleotide at one NBD, and almost complete inhibition of ATPase activity [114]. This mutation abolished enzymatic activity by inhibiting formation of the catalytic transition state. Mutations of Ser (S430/S1073) or Lys (K429/K1072) residues in the Walker A motifs were also shown to be involved in reducing catalytic turnover, and allowed ATP binding, but inhibited occlusion [115]. The Q-loop is thought to be involved in communication between the substrate binding pocket and the catalytic sites, and mutations in the Q-loop Gin residues (Q471/Q1114) greatly reduced the stimulation of ATPase activity by verapamil [116]. Mutation of the conserved His residue in the H-loop (H662A) of HlyB resulted in a loss of ATPase activity, and has been proposed to be the “linchpin” of catalytic activity [117].

The TMDs of ABC proteins contain α -helical motifs that are embedded in the surface of the NBDs, at the interface between the helical and catalytic subdomains, and are essential for transmitting conformational changes between the NBDs and

TMDs. These coupling helices share little sequence similarity, but when bound to the NBDs their structures are very similar when superimposed upon one another [15,109]. The binding of the coupling helices to the NBDs differs for ABC importers and exporters. In exporters (Sav1866 and MsbA), the TMD of one subunit interacts with the NBD of the opposing subunit, resulting in tight association of the NBDs, and a twisted conformation [17,80]. In contrast, the coupling helices of ABC importers (ModB₂C₂A, BtuCD, HI1470/71, maltose permease) are not swapped with the NBDs, resulting in a large gap at the centre of the transporter [15,109]. The coupling helices provide evidence for a common transport mechanism for all ABC proteins. The binding of substrate to an ABC protein, which occurs through interactions with an extracellular binding protein in importers, facilitates ATP hydrolysis by bringing the NBDs and coupling helices together, resulting in the protein transitioning from an inward-facing conformation to an outward-facing conformation [81,109]. ATP hydrolysis is thought to cause a reorientation of the TM helices that disrupts protein-substrate interactions, and results in substrate translocation. According to this model, translocation would occur in importers after the release of ADP and P_i resets the protein back to the inward-facing conformation [109], whereas in exporters, translocation would occur before the release of ADP and P_i.

The binding to Pgp of a variety of nucleotides has been characterized, including ADP, ATP, their fluorescent derivatives 2'(3')-O-(2,4,6-trinitrophenyl)adenosine 5'-diphosphate (TNP-ADP) and 2'(3')-O-(2,4,6-trinitrophenyl)adenosine 5'-triphosphate (TNP-ATP), as well the non-hydrolysable nucleotide analogues AMP-PNP and ATP- γ -S. The binding affinities of ADP, ATP, and AMP-PNP to Pgp are all quite similar (K_d 0.2- 0.4 mM) [101, 118], whereas the fluorescent nucleotides TNP-ADP and TNP-ATP bind to Pgp with a much higher affinity (K_d ~5 μ M) [119]. The tight binding of TNP-labelled nucleotides is likely due to interactions of the hydrophobic trinitrophenyl group with nonpolar regions of Pgp. The non-hydrolysable analogue ATP- γ -S binds to Pgp with an even higher affinity than the fluorescent nucleotides (K_d 5 μ M), and when bound to the protein may induce the formation of the occluded state [120]. ATP occlusion had previously been demonstrated only for catalytically deficient Pgp mutants. Purified Pgp generally demonstrates a high basal level of ATPase activity in the absence of substrate, although protein preparations from some

groups have very low basal ATPase activity, and need to be reactivated by adding lipids or reducing agents. These preparations often show a much higher fold-increase in drug stimulated ATPase activity due to an underestimation of the true potential basal activity [121].

It is thought that hydrolysis of ATP at the NBDs of Pgp occurs by an alternating sites mechanism, in which only one of the two catalytic sites is active at any time [122]. Communication between the two NBDs is facilitated by the D-loop, which enables alternating catalysis of ATP by transmitting information between the NBDs via the H-loop [117]. Both catalytic sites need to be functional for transport to occur as indicated by studies in which ATPase activity was abolished when mutations were made at one of the NBDs [123]. Pgp is able to bind two ATP molecules at once [124,125], but there has been debate over whether one or two molecules of ATP are hydrolyzed during the transport cycle. There has been a proposal that there are two rounds of ATP hydrolysis, with the first round driving substrate translocation, and the other responsible for resetting the protein for subsequent transport [126,127]. However, it has been demonstrated that there is an asymmetric occlusion of ATP during the catalytic cycle, with a stoichiometry of 1 [115,128] which would indicate that one ATP is hydrolyzed per transport cycle, as proposed in the original alternating sites mechanism.

1.4 Transport Mechanisms of Pgp

1.4.1 Hydrophobic vacuum cleaner and flippase models

The majority of Pgp substrates are hydrophobic, indicating they likely first partition into the membrane bilayer before interacting with the protein. The location of the substrate binding sites of Pgp have been mapped in the cytoplasmic leaflet of membrane bilayer [76,77], supporting the idea that Pgp substrates must first partition into the membrane before they can bind to the protein. Many Pgp substrates have high lipid-water partition coefficients (P_{lip}), which is consistent with this idea. Drugs with a high P_{lip} tend to have a high affinity (low K_d) for binding to Pgp [129]. Once drugs have partitioned into the membrane, they move into the substrate binding pocket of Pgp in a process that is nearly isoenergetic [130], possibly through gates at the interface of the two TMDs, formed by TM helices 2 and 11 at one end of Pgp, and helices 5 and 8 at the opposite end [105].

Two similar, but distinct mechanisms have been proposed for Pgp-mediated drug efflux; the hydrophobic vacuum cleaner model, and the flippase model [131]. It has been proposed that Pgp acts as a hydrophobic vacuum cleaner that binds drugs somewhere within the membrane and expels them to the extracellular medium. The flippase model is compatible with the hydrophobic vacuum cleaner model, and proposes that Pgp is a flippase that binds drugs in the cytoplasmic leaflet of the membrane and flips them to the extracellular leaflet. Attempts to distinguish between these two models have been inconclusive, as it is difficult to determine whether drugs are transported directly to the extracellular medium, or merely to the extracellular leaflet of the membrane, because drugs can partition very rapidly between the two locations.

1.4.2 Catalytic cycle

The catalytic cycle of Pgp involves the coupling of ATP binding and hydrolysis with substrate translocation across the cell membrane. Reactions taking place at the NBDs during the catalytic cycle include ATP binding and formation of a nucleotide sandwich dimer, followed by ATP hydrolysis, P_i dissociation, and finally ADP dissociation. For substrate translocation, drugs bind in the substrate binding pocket located in the inner leaflet, and conformational changes in the TMDs transport the substrate across the membrane where it is released. ATP binding, ATP hydrolysis and the release of ADP/ P_i have all been shown to result in conformational changes in the protein [132], suggesting that energy is released at each of these steps. Crosslinking studies have shown that substrate binding induces changes in the packing of the TMDs [73]. Covalent coupling of the TMDs reversibly abolished ATPase activity [133], suggesting that nucleotide hydrolysis at the NBDs is coupled to substrate translocation via rotation or displacement of the TMDs.

How ATP binding and hydrolysis drives the transport of Pgp substrates has been the subject of much debate. The binding of drugs can result in stimulation or inhibition of the ATPase activity of Pgp, with some drugs showing a biphasic pattern, with stimulation at low concentrations and inhibition at higher concentrations [134]. The presence of both a high-affinity stimulatory drug binding site, and a low-affinity inhibitory drug-binding site could explain the biphasic pattern [135]. Drugs that stimulate ATPase activity cause the Walker A residues of one half of Pgp to move closer to the LSGGQ motif of the other half [136], and promote occlusion of ATP at

one NBD [115], facilitating ATP hydrolysis. The establishment of a nucleotide sandwich dimer appears to be an important step in the catalytic cycle of Pgp, but there is still debate as to whether it is the binding of ATP, or ATP hydrolysis itself that drives the transport of substrates, and whether drug binding stimulates ATP binding and dimerization of the NBDs.

One proposed model for drug translocation by Pgp is the ATP switch model [137], in which resting state Pgp would have high affinity for substrates and low affinity for ATP. Substrate binding initiates communication with the NBDs, resulting in the binding of two ATP molecules. ATP binding induces NBD dimerization, with corresponding changes in the TMDs that result in substrate translocation by exposing the substrate to the extracellular environment, where the TMDs have low affinity for substrate. ATP hydrolysis at one or both NBDs, followed by release of ADP and P_i , resets Pgp back to its resting state. Although this model claims to be supported by available biochemical data, it makes numerous assumptions based on the photoaffinity labelling technique, which has been shown to be an unreliable method for measuring binding affinity [138]. Pgp drug substrates are clearly not required for NBD dimerization, as Pgp can bind and hydrolyze ATP in the absence of substrates [121]. It has also been demonstrated that the rate-limiting step of transport is ATP hydrolysis, which is associated with a reorientation of the drug binding site from a high-affinity state to a low affinity state [139], indicating that ATP binding does not cause substrate translocation as proposed in this model. While the ATP switch model attempts to provide a generalized transport mechanism for all ABC proteins, it is inconsistent with biochemical data available for Pgp, and does not adequately explain the catalytic cycle of this protein.

Orthovanadate (V_i) is a phosphate analogue that has helped give insight into the catalytic cycle of Pgp. V_i can reversibly replace P_i in a single active site after ATP hydrolysis, trapping Pgp in a stable complex. The vanadate trapped Pgp-ADP- V_i - M^{2+} (where M^{2+} is a divalent cation) still has one free NBD, but displays no ATPase activity [140], and is thought to have a structure that resembles the catalytic transition state. The complex is stable for >3 h when trapped in the presence of Co^{2+} [125], allowing for detailed studies with fluorescence spectroscopy, before slow dissociation of V_i , and subsequently ADP, results in full restoration of ATPase activity. Vanadate-trapped Pgp has been shown to have a substrate binding affinity

similar to that of native Pgp, indicating that ATP hydrolysis, rather than the release of ADP, resets the transporter back to its resting state [141]. Crosslinking studies show that the vanadate-trapped state has different residues accessible to crosslinkers compared to nucleotide-free Pgp [142], suggesting that although Pgp-ADP-V_i-M²⁺ has normal affinity for substrates, some TM helix rotations are still required for the protein to regain its native conformation [143].

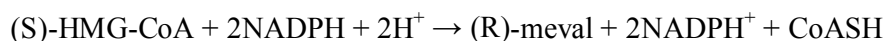
Detailed biochemical studies of Pgp using spin-labelled substrates, and thermodynamic analysis at different stages of the catalytic cycle, led to the proposal of the partition model, in which Pgp has two distinct transition states [121]. One transition state corresponds to basal ATPase activity that is uncoupled from drug translocation, and the other state corresponds to coupled drug transport activity. If there is sufficient drug present, Pgp will partition into the drug-coupled transport cycle, in which substrate binding is followed by the binding of two ATP molecules, with occlusion and hydrolysis of one ATP by an alternating sites mechanism [122]. When no drug is present, and a second molecule of ATP binds, then the protein will partition into the uncoupled basal cycle. The rate-limiting step for both the basal cycle and drug-coupled cycle is ATP hydrolysis, and the energy released from hydrolysis of one ATP molecule is sufficient to forcibly rehydrate a bound drug molecule [121]. ATP hydrolysis is proposed to move substrates from a drug loading “ON-site” in the inner leaflet with high affinity for substrate, to a drug-unloading “OFF-site” in the extracellular leaflet with low affinity for substrate, resulting in transport of drug across the membrane. For drug substrates that show inhibition of ATPase activity at higher concentrations, free energy analysis demonstrated that this is not the result of a separate rate-limiting step, but likely the result of inhibition of drug release from the low affinity OFF-site. However, studies showing a permanent increase in ATPase activity after covalent crosslinking of methanethiosulfonate (MTS)-verapamil to the drug binding pocket suggest that drug release from the “ON-site” is not required for ATPase stimulation [144].

The drug-coupled ATPase activity of various drugs displayed a linear free energy relationship, indicating that all drugs have the same rate-limiting transition step during the transport cycle. Basal ATPase activity has a clearly different free energy relationship from drug-coupled activity, suggesting that basal activity is not the result of either transport of an unidentified substrate, or nonspecific lipid-flipping, as

previously suggested [145]. Each drug makes unique molecular interactions with the transition state, and has a different intrinsic k_{cat} value. Drugs that require fewer molecular rearrangements to achieve the transition state are transported faster, and therefore have a higher level of drug-coupled ATPase activity. This model explains how some drugs appear to stimulate ATPase activity, whereas others appear to have no effect. If the drug-coupled ATPase activity for a particular substrate is higher than the intrinsic basal ATPase activity, then biochemical assays will indicate that the drug causes a stimulation of ATPase activity. The partition model is currently the only model in the literature that can account for most of the kinetic data available for Pgp [146], and may explain the complex relationship between the catalytic and drug transport cycles of this enzyme.

1.5 HMG-CoA Reductase Inhibitors (Statins)

Elevated cholesterol levels are a primary risk factor for coronary artery disease. This disease is a major problem in developed countries. Dietary changes and drug therapy reduce serum cholesterol levels and dramatically decrease the risk of stroke and overall mortality. Inhibitors of HMGR, commonly referred to as statins, are effective and safe drugs that are widely prescribed in cholesterol-lowering therapy. In addition to lowering cholesterol, statins appear to have a number of additional effects, such as the nitric oxide-mediated promotion of new blood vessel growth [147] stimulation of bone formation [148], protection against oxidative modification of low-density lipoprotein, as well as anti-inflammatory effects and a reduction in C-reactive protein levels [149]. Based on the accumulation of evidence obtained *in vitro* and in clinical settings, statins are now being tried for other diseases, including Alzheimer's disease, cancer, and osteoporosis [150]. All statins curtail cholesterol biosynthesis by inhibiting the committed step in the biosynthesis of isoprenoids and sterols [151]. This step is the four-electron reductive deacylation of HMG-CoA to CoA and mevalonate. It is catalyzed by HMGR in a reaction that proceeds as follows;



where NADP^+ is the oxidized form of nicotinamide adenine dinucleotide, NADPH is the reduced form of NADP^+ , and CoASH is the reduced form of CoA.

Several statins are available or in late-stage clinical development (Figure 1.4). All share an HMG-like moiety, which may be present in an inactive lactone form. *in vivo*, these prodrugs are enzymatically hydrolyzed to their active hydroxy-acid forms [151]. The statins share rigid, hydrophobic groups that are covalently linked to the HMG-like moiety. Lovastatin, pravastatin, and simvastatin resemble the substituted decalin-ring structure of compactin (also known as mevastatin). Fluvastatin, cerivastatin, atorvastatin, and rosuvastatin are fully synthetic HMGR inhibitors with larger groups linked to the HMG-like moiety. The additional groups range in character from very hydrophobic (e.g., cerivastatin) to partly hydrophobic (e.g., rosuvastatin). All statins are competitive inhibitors of HMGR with respect to binding of the substrate HMG-CoA, but not with respect to binding of NADPH [152]. The K_i (inhibition constant) values for the statin-enzyme complexes range between 0.1 to 2.3 nM [151], whereas the Michaelis constant, K_m , for HMG-CoA is 4 μ M [153].

As statins come to be used more frequently to treat complicated diseases, one should use them more carefully paying attention to drug-drug interactions, which raise the risk of adverse events [154]. In 2001, cerivastatin was withdrawn from the market because of rhabdomyolysis found especially in patients coprescribed gemfibrozil. It has been proved that gemfibrozil elevated cerivastatin concentration with 5.6-fold for AUC of parent form and 4.4-fold for that of lactone form [155].

1.6 Role of P-glycoprotein on Statin Pharmacokinetics

Atorvastatin [156] (acid [157-160], methyl ester [157], and lactone [157,161] forms), lovastatin (lactone form) [156,157,159,161,162] and simvastatin (acid [159] and lactone forms) [156,157,159,161,163] inhibit P-gp substrate transport in a concentration-dependent manner, [156-158,160] with high concentrations of atorvastatin needed in some studies [156,159,160].

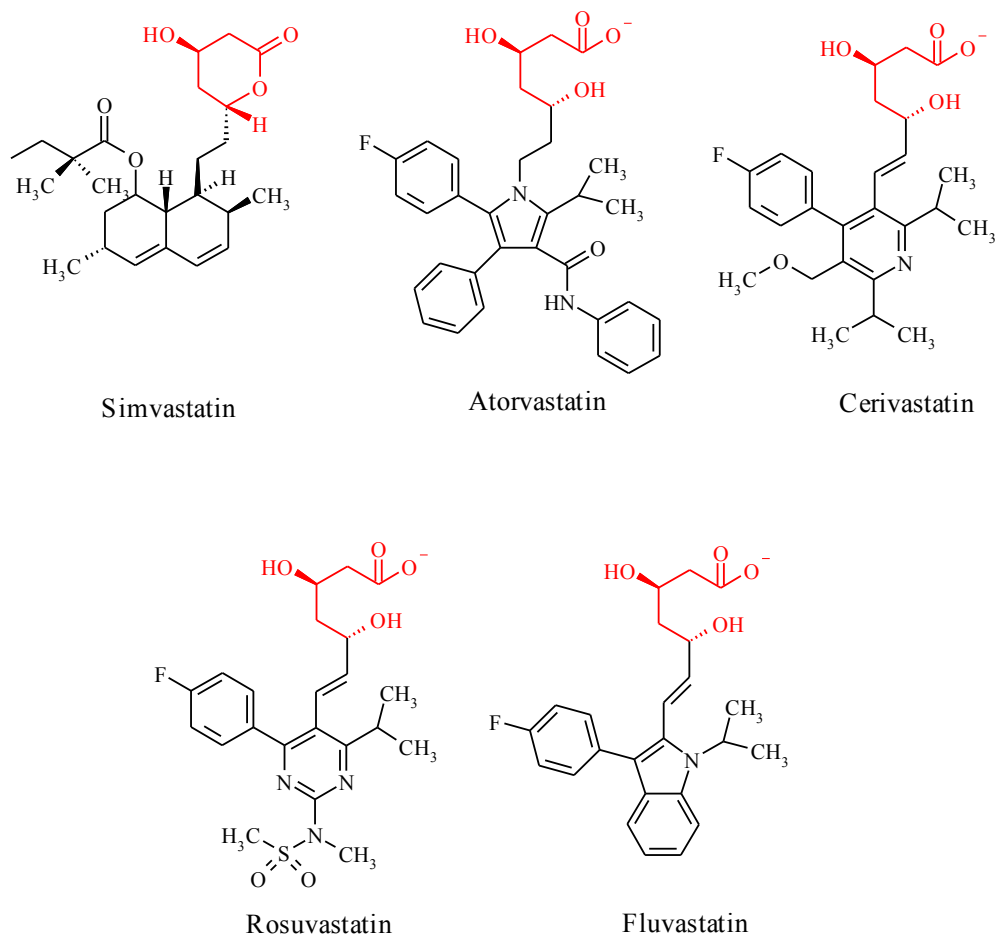


Figure 1.4 : Statins: Structural formulas of statin inhibitors and the enzyme substrate HMG-CoA. The HMG-like moiety that is conserved in all statins is colored in red

Drug interactions have been reported between statins and Pgp substrates or inhibitors, including St. John's wort, digoxin, diltiazem, verapamil, itraconazole, grapefruit juice, cyclosporine, mibefradil, erythromycin, and clarithromycin [164]. Of interest, great overlap exists between agents that are both CYP3A4 and Pgp substrates or inhibitors [165,166]. With the exception of digoxin, all other Pgp substrates or inhibitors are also CYP3A4 modulators [166,167]. Statins are generally regarded as CYP3A4 substrates; however, neither pravastatin nor rosuvastatin has been shown to be metabolized by CYP3A4 [167-169]. Pravastatin is enzymatically broken down in liver cells into inactive metabolites [168], and fluvastatin is metabolized predominantly by CYP2C9 [167]. An *in vitro* study showed that rosuvastatin was neither a substrate nor an inhibitor of CYP3A4 [169]. Coincidentally, fluvastatin (although partially metabolized by CYP3A4), pravastatin, and rosuvastatin have not

been shown to be a substrate or inhibitor of Pgp [164]. How much the drug interactions with simvastatin, lovastatin, and atorvastatin are due to CYP3A4 or Pgp modulation is unknown. However, since data suggest that these statins are Pgp substrates, both CYP3A4 and Pgp modulation may be involved in the interaction, causing an increase in serum concentrations of the respective statin. There is great opportunity to explore the precise mechanisms of these drug interactions. Interactions that were once thought to be purely related to CYP3A4 interactions may also be at least partly explained by Pgp-mediated interactions.

1.7 Aim of The Study

The purpose of this study is to investigate the interactions of Pgp with statins by the aid of molecular dynamic simulation and by using Atorvastatin as a model compound.

2. METHODOLOGY

2.1 Molecular Dynamics Simulation

Biomolecular dynamics occur over a wide range of scales in both time and space, and the choice of approach to study them depends on the question asked. Molecular simulation is far from the only theoretical method; when the aim is to predict, e.g., the structure and/or function of proteins rather than studying the folding process, the best tool is normally bioinformatics that detect related proteins from amino acid sequence similarity; and, for computational drug design, often it is much more productive to use statistical methods such as quantitative structure–activity relationship (QSAR) instead of spending billions of CPU hours to simulate binding of thousands of compounds.

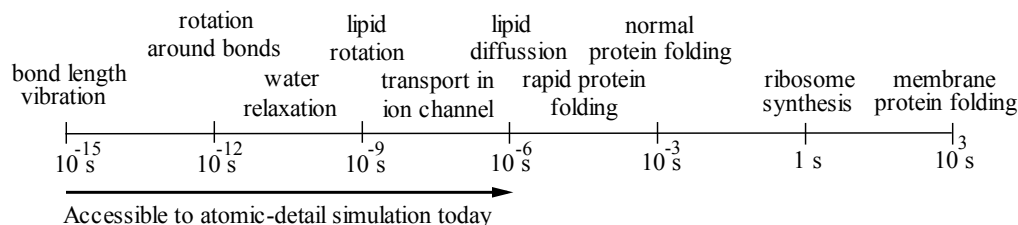


Figure 2.1 : Range of time scales for dynamics in biomolecular systems: Although the individual time steps of molecular dynamics is 1 to 2 fs, parallel computers make it possible to simulate on a microsecond scale, and distributed computing techniques can sample even slower processes, almost reaching milliseconds [170].

The most important point of simulations is that they provide a way to test whether theoretical models predict experimental observations. As an example, simulations of ion channels cannot compete with experiments when it comes to measuring ion currents, but they have been useful to explain why some ions pass whereas others are blocked. Similarly, simulations can provide detail not accessible through experiments, for instance, pressure distributions inside membranes. Further, structural refinement and energy minimizations are regularly used to improve both experimental and predicted protein structures, and drug design is moving toward

more accurate models, even including large-scale simulations for free energy screening.

Ideally, the time-dependent Schrödinger equation should be able to predict all properties of any molecule with arbitrary precision *ab initio*. However, as soon as more than a handful of particles are involved, it is necessary to introduce approximations. For most biomolecular systems, we, therefore, choose to work with empirical parameterizations of models instead; for instance, classic Coulomb interactions between pointlike atomic charges rather than a quantum description of the electrons. These models are not only orders of magnitude faster, but because they have been parameterized from experiments, they also perform better when it comes to reproducing observations on a microsecond scale (see Figure 2.1), rather than extrapolating quantum models 10 orders of magnitude. The first molecular dynamics simulation was performed as late as 1957 [171], although it was not until the 1970s that it was possible to simulate water [172] and biomolecules [173].

2.2 Theory

Macroscopic properties measured in an experiment are not direct observations, but averages over billions of molecules representing a statistical mechanics ensemble. This has deep theoretical implications, which are covered in great detail in the literature [174,175], but, even from a practical point of view, there are important consequences. 1) It is not sufficient to work with individual structures, but systems have to be expanded to generate a representative ensemble of structures at the given experimental conditions, e.g., temperature and pressure. 2) Thermodynamic equilibrium properties related to free energy, such as binding constant, solubilities, and relative stability, cannot be calculated directly from individual simulations. 3) For equilibrium properties (in contrast to kinetic), the aim is to examine the ensemble of structures, and not necessarily to reproduce individual atomic trajectories.

The two most common ways to generate statistically faithful equilibrium ensembles are Monte Carlo and molecular dynamics simulations; the latter also has the advantage of accurately reproducing kinetics of non-equilibrium properties such as diffusion or folding times. When a starting configuration is very far from equilibrium, large forces can cause the simulation to crash or distort the system, and, in this case, it is necessary to start with energy minimization of the system before the

molecular dynamics simulation. In addition, energy minimizations are commonly used to refine low-resolution experimental structures.

All classic simulation methods rely on more or less empirical approximations called force fields [176-179] to calculate interactions and evaluate the potential energy of the system as a function of point like atomic coordinates. A force field consists of both the set of equations used to calculate the potential energy and forces from particle coordinates, as well as a collection of parameters used in the equations. For most purposes, these approximations work well, but they cannot reproduce quantum effects such as bond formation or breaking.

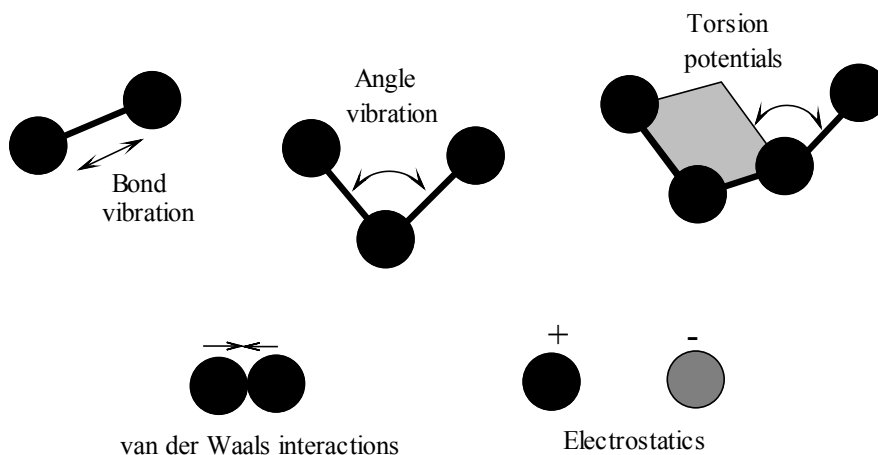


Figure 2.2 : Examples of interaction functions in modern force fields: Bonded interactions include covalent bond-stretching, angle-bending, torsion rotation around bonds and out-of-plane or “improper” torsions (not shown). Non-bonded interactions are based on neighborlists and consist of Lennard-Jones attraction and repulsion as well as Coulomb electrostatics.

All common force fields subdivide potential functions into two classes. Bonded interactions cover covalent bond-stretching, angle-bending, torsion potentials when rotating around bonds, and out-of-plane “improper torsion” potentials, all which are normally fixed throughout a simulation (see Figure 2.2). The remaining nonbonded interactions consist of Lennard-Jones repulsion and dispersion as well as Coulomb electrostatics. These are typically computed from neighbour lists updated every 5 to 10 steps.

Given the potential and force (negative gradient of potential) for all atoms, the coordinates are updated for the next step. For energy minimization, the steepest

descent algorithm simply moves each atom a short distance in the direction of decreasing energy, while molecular dynamics is performed by integrating Newton's equations of motion (see Equation 2.1) [180].

$$\begin{aligned} F_i &= -\frac{\delta V(r_1, \dots, r_N)}{\delta r_i} \\ m_i \frac{\delta^2 r_i}{\delta t^2} &= F_i \end{aligned} \tag{2.1}$$

The updated coordinates are then used to evaluate the potential energy again, as shown in the flowchart of Figure 2.3.

Typical biomolecular simulations use periodic boundary conditions to avoid surface artifacts, so that a water molecule that exits to the right reappears on the left; if the box is sufficiently large, the molecules will not interact significantly with their periodic copies. This is intimately related to the non-bonded interactions, which ideally should be summed over all neighbors in the resulting infinite periodic system. Simple cut-offs can work for Lennard-Jones interactions that decay very rapidly, but, for Coulomb interactions, a sudden cut-off can lead to large errors. One alternative is to "switch off" the interaction before the cut-off, but a better option is to use particle mesh Ewald summation (PME) to calculate the infinite electrostatic interactions by splitting the summation into short- and long-range parts [181]. For PME, the cut-off only determines the balance between the two parts, and the long-range part is treated by assigning charges to a grid that is solved in reciprocal space through Fourier transforms.

Cut-offs and rounding errors can lead to drifts in energy, which will cause the system to heat up during the simulation. To control this, the system is normally coupled to a thermostat that scales velocities during the integration to maintain room temperature. Similarly, the total pressure in the system can be adjusted through scaling the simulation box size, either isotropically or separately in x, y, and z dimensions.

The single most demanding part of simulations is the computation of non-bonded interactions, because millions of pairs have to be evaluated for each time step. Extending the time step is, thus, an important way to improve simulation performance, but, unfortunately, errors are introduced in bond vibrations already at 1 fs. However, in most simulations, the bond vibrations are not of interest per se, and

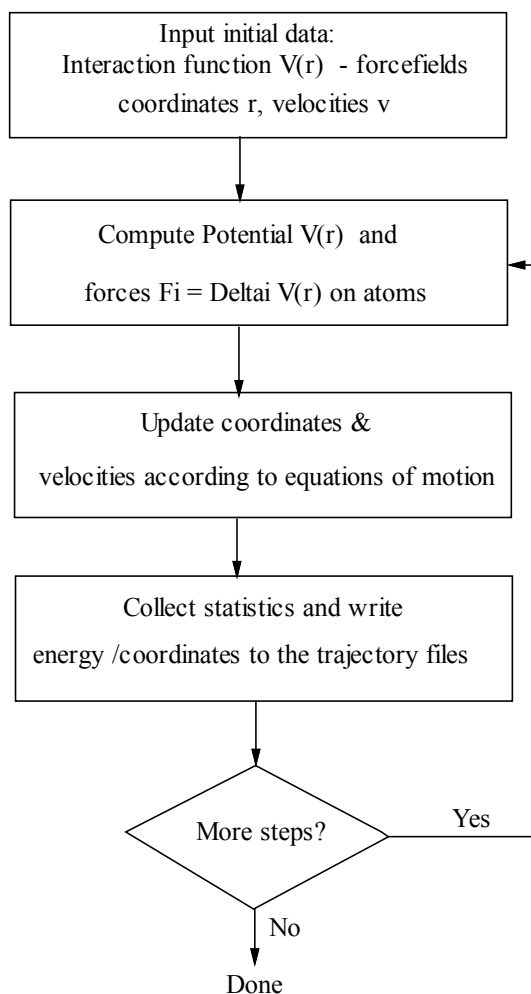


Figure 2.3 : Simplified flowchart of a typical molecular dynamics simulation: The basic idea is to generate structures from a natural ensemble by calculating potential functions and integrating Newton's equations of motion; these structures are then used to evaluate equilibrium properties of the system. A typical time step is on the order of 1 or 2 fs!

can be removed entirely by introducing bond constraint algorithms such as SHAKE [182] or LINCS [183]. Constraints make it possible to extend time steps to 2 fs, and fixed-length bonds are likely better approximations of the quantum mechanical ground state than harmonic springs.

2.2.1 Potential energy function

The backbone of the classical simulations is the potential energy function, a relation that expresses the energy of a molecular system as a function of its atomic coordinates [184].

A typical potential energy function has the form:

$$V_{total} = \sum_{bonds} \frac{1}{2} k^b (b - b_{eq})^2 + \sum_{angles} \frac{1}{2} k^\theta (\theta - \theta_{eq})^2 + \sum_{\substack{proper \\ dihedral}} k^\phi [1 + \cos(n\phi - \phi^0)] + \sum_{\substack{i < j \\ Len-Jon}} \frac{A_{ij}}{r_{ij}^{12}} - \frac{B_{ij}}{r_{ij}^6} + \sum_{\substack{i < j \\ Coulomb}} \frac{q_i q_j}{4\pi\epsilon_0 r_{ij}} \quad (2.2)$$

The first three terms are associated with covalently connected atoms, while the last two terms are for non-covalent or non-bonded interaction between atoms. The first term is a summation over energies associated with bond stretching between two covalently bonded atoms (1-2, two-body interactions), the second term represents the bending of bond angles (1-3 three-body interactions) while the third term represents torsions (1-4, four body interactions). In the fourth term, van der Waals interactions are described by a Lennard-Jones potential between atoms separated by distance r_{ij} . The fifth term is associated with electrostatic interactions, described as partial point charges interacting via Coulomb's law. Non-bonded pair interactions involving atoms that are covalently linked by one or a chain of two bonds (e.g. pairs 1-2 and 1-3) are normally excluded from the fourth and fifth terms. Terms in the equation are optimized to describe physical interactions that determine the structure and dynamic properties of the molecular system. Nuclei and electrons are treated together as spherical particles (atoms) with a net point charge. Atomic radii are determined from experimental structural data while bonds connecting atoms are modelled as harmonic springs with the ability to stretch, bend and twist as illustrated in Figure 2.2.

Equation (2.2) represents the basic functional form of the potential energy function. Variants of this equation may have additional terms such as: an improper dihedral term to prevent out-of-plane distortions, mixed terms that directly couple stretching and bending in adjacent bonds, special hydrogen-bond terms to account for electronic polarizability etc [185]. These extensions are normally meant to increase accuracy or to tailor the function for specialized applications. The quest for increased

accuracy is, however, normally associated with increased computational cost. The values for bond lengths b , bond angles θ , torsion angles ψ and distance between atoms r_{ij} , are obtained from experimental X-ray or NMR structures or from modeled structures. The rest of the parameters in Equation (2.2) are optimized to reproduce experimentally known properties of the system or *ab initio* quantum data on small molecules. Experimental data used in fitting parameters include, densities, enthalpies of vaporization and free energies of solvation. The potential energy function, together with its associated set of parameters, constitute a “force-field”. Commonly used force-fields for simulating biomolecules include AMBER [186], CHARMM [177], GROMOS [187] and OPS [188]. Naturally, the choices of the force-field should be guided by the type of molecular system for which it has been parameterized.

Following the choice of an appropriate force-field, the next task is to generate a set of low energy configuration of the molecular system to be used in statistical mechanical evaluation of macroscopic properties.

2.3 Simulation Detail

2.3.1 Simulation system design

The initial systems (see Table 2.1 and Figure 2.4) was set up to explore the conformational dynamics of Pgp, an approximation of the physiological environment, whereby the entire protein is inserted into a solvated lipid (dimyristoyl phosphatidylcholine, DMPC) bilayer in a box of water. Then the system was explored with and without different substrates. For simulation ALLM (N-acetyl-lue-leu-methinonal), AFMRF (N-acetyl-phe-met-arg-phe-al) linear peptide and lactone atorvastatin is used as substrates.

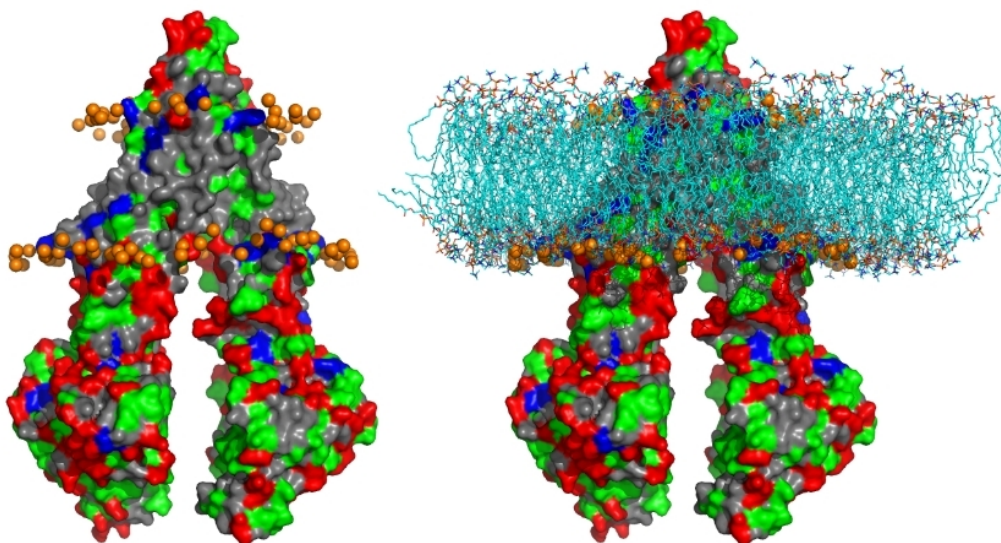


Figure 2.4 : Simulation system: Pgp is shown in surface representation. The Pgp complex is embedded in a DMPC bilayer, with headgroup phosphorus atoms in orange and the hydrophobic tails of the lipids in cyan. The hydrophobic residues of Pgp are colored gray. TYR and TRP (red) residues that positioned between and lipid and aqua phase charged residues (blue) that are generally positioned in aqua phase.

Table 2.1: Summary of simulations

Simulation	Components	Number of atoms	duration restrained (ns)	duration unrestrained (ns)
APO	Pgp	~220,000	1.2 ns	10 ns
ALLM	Pgp + MgATP + ALLM	~220,000	1.2 ns	10 ns
AFMRF	Pgp + MgATP + AFMRF	~220,000	1.2 ns	10 ns
AFMRF-noATP	Pgp + AFMRF	~220,000	1.2 ns	10 ns
LACAVA	Pgp + MgATP + Lactone Atorvastatin	~220,000	1.2 ns	10 ns

2.3.2 System preparation and simulations

Coordinate (PDB code 3G60 [16]) for Pgp were used and downloaded from the Protein Data Bank [189]. The only modification from the downloaded coordinates was the removal of the bonded inhibitor molecules from the Pgp structure.

A pre-equilibrated DMPC bilayer of 128 lipid bilayer [190] is used to construct 512 bilayer. The TMDs were inserted in this bilayer and oriented using bands of charged

residues to determine the optimal position of the protein relative to the bilayer. The protein is then oriented in such a way that its hydrophobic belt is aligned with the non-polar lipid tails [191]. DMPC molecules overlapping the protein were removed with *g_membed* [192] application, and the resultant Pgp/bilayer system was solvated, energy-minimized, and equilibrated for 5 ns, with the non-H atoms of the Pgp restrained (force constant) $1000 \text{ kJ mol}^{-1}\text{nm}^{-1}$) in order to allow a relaxation of the packing of lipids around the protein.

Polar hydrogens were added to the crystal structure of Pgp. A doubly protonated state was chosen for the side chain of each histidine residue in H-Switch of NBD. Default protonation states were assumed for all other residues.

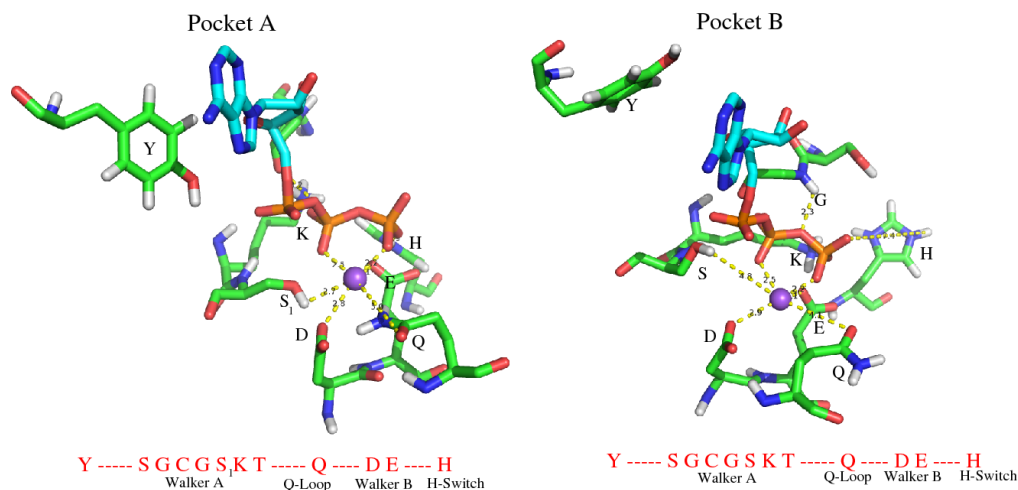


Figure 2.5 : Docking of lactone atorvastatin: This figure represents binding pocket of lactone atorvastatin in Pgp. This binding pocket is found by docking and nearly same for all other used substrates.

In order to generate the Pgp and substrate complex, it was necessary to dock the substrate into Pgp. Before docking, substrate was positioned in place of inhibitor position according to crystal structure. After this positioning of substrate, Autodock and Autock Vina tools [193,194] were used to dock substrates.

Mg^{2+} -ATP was docked into the NBDs using the MJ0796 NBD dimer structure (PDB code 1L2T) as a template. The Na-ATP coordinates from MJ0796 were superimposed onto each Pgp by least-squares fitting of residues from the Walker A and Walker B motifs and the Q-loop. It was then assumed that the Mg^{2+} ion binds to the same coordinates as the Na^+ ion. In the default ATP force field the γ -phosphate is singly protonated. We modified this by removing the hydrogen from the γ -phosphate

and redistributing the partial charges evenly over the phosphate oxygen atoms such that the overall charge of the MgATP is $-2e$.

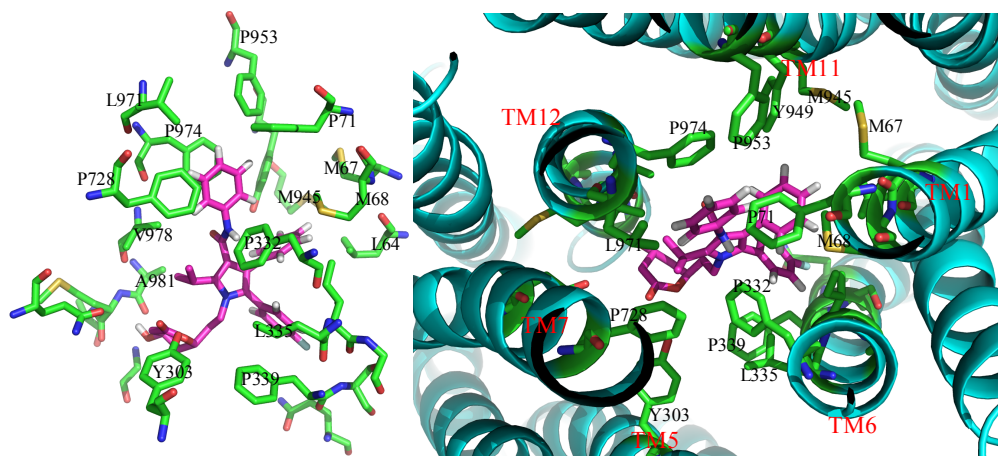


Figure 2.6 : ATP Docking: Each ATP molecules are docked manually by represent characteristic all ABC transporters. All motifs have a role in positioning ATP molecule is represented in figure. Mg atom and coordination shell hydrogen bonding are represented by yellow dots.

All energy minimization was performed using 100 steps of the steepest descents algorithm. Equilibration was performed using harmonic restraints on the protein non-H atoms (and ATP when present) (force constant) $1000 \text{ kJ mol}^{-1} \text{ nm}^{-1}$), a Berendsen thermostat [195], and pressure maintained at 1 bar by a Berendsen barostat [195]. The unrestrained production runs were performed with a Nose-Hoover thermostat ([196-197] and pressure maintained at 1 bar by a Parrinello-Rahman barostat [198]. The simulations were run in the NPT ensemble and at a temperature of 310 K. Particle mesh Ewald (PME) was used to treat long-range electrostatics [199], and the single point charge (SPC) water model [200] was used for the solvent. Chloride anions were positioned randomly among the solvent to neutralize the system. The integration time step was 2 fs, and coordinates were saved every 5 ps for subsequent analysis. The LINCS algorithm was used to restrain all bond lengths [183].

Simulations were run and analyzed using the GROMACS v. 4.0.5 (<http://www.gromacs.org>) molecular dynamics simulation package [201-203] with the GROMOS96 united-atom forcefield [178,187]. Lipid parameters were based on those described in [190]. Pore profiles were calculated using CAVER [204]. 3D graphics were produced using VMD [205] and PyMol [206].

2.4 Analysis Method

The positions and velocities of every atom of a simulation system are specified for every time step by the simulation trajectory. The structural changes of a protein can thus be obtained from such a trajectory, and are characterized by the methods introduced below.

2.4.1 Root mean square deviation

The root mean square deviation (RMSD) of a structure with atomic coordinates r_i with respect to a reference structure with its atoms coordinates r_i^0 yields a quantitative measure for the structural difference between both,

$$RMSD = \sqrt{\frac{1}{N} \sum_{i=1}^N (r_i - r_i^0)^2} \quad (2.3)$$

The definition of the RMSD requires the rotation and translation of the structure towards its best fit to the reference structure. The calculation of an appropriate RMSD of a protein's structure along its trajectory with respect to its crystal structure, e.g., yields a measure for conformational changes. Typically, an RMSD of 2–3 Å is caused by thermal fluctuations, whereas larger values point towards conformational changes.

To obtain information about the globular motion of the structure, a subset of atoms from the system is chosen for the calculation of the RMSD via Equation (2.3). This subset consists out of the amino acid backbone atoms, due to the noise induced by the fluctuations of amino acid side-chains. However, if a certain region in the protein is expected to contribute strongly to the total RMSD, a subset of atoms from that particular region can be used to calculate a more specific RMSD of that region.

Even though the RMSD can indicate general motions or conformational changes, the specific motions in phase space cannot be exactly determined. It is, therefore, not possible to correlate the globular motions of a protein from two or more independent trajectories by their respective time resolved RMSD.

2.4.2 Principal component analysis

One major technique to extract and classify information about large conformational changes from an ensemble of protein structures generated either experimentally or theoretically, is principal component analysis (PCA). A detailed mathematical description of PCA is given in ref. [180,207]. Principal component analysis is based on the observation that the largest part of positional fluctuations in biomolecules, like proteins, occurs along a small subset of collective degrees of freedom. The presence of a large number of internal constraints, defined by the atomic interactions in a biomolecule, leads to the dominance of this small subset of degrees of freedom (essential subspace) in the molecular dynamics of a protein. In particular, these interactions range from the strong covalent bonds to the weaker non-bonded interactions. PCA identifies the collective degrees of freedom that most contribute to the total amount of fluctuations. Typically, a small subset of 5–10% of the total degrees of freedom accounts for more than 90% of the total fluctuations within a protein [207-209].

In general, PCA can be regarded as a multi-dimensional linear least squares fit procedure in configuration space. After fitting each configuration to a reference structure, the covariance matrix of the atoms positional fluctuations is build and diagonalized,

$$C = \left\langle (R(t) - \langle R \rangle)(R(t) - \langle R \rangle)^T \right\rangle \quad (2.4)$$

where $R(t)$ resembles the fitted ensemble (e.g. from a MD trajectory) of internal motions and $\langle \rangle$ an ensemble average. Here, R is a column vector of size $3N$, describing the coordinates of N atoms, and thus representing every structure of the ensemble. Because the collective motions of a protein are described very well by their backbone motions, the covariance matrix was made up by the proteins backbone atoms in this work. The sym-metric $3N \times 3N$ matrix C is diagonalized by an orthogonal coordinate transformation D , containing the eigenvalues λ_i of matrix C . The i th column of D contains the normalized eigenvector, i.e. principal component, μ_i of matrix C corresponding to λ_i .

The eigenvalues λ_i describe the mean square fluctuations along the respective eigenvector μ_i . Hence, they contain each principal component's contribution to the

total fluctuation. Sorting the eigenvectors μ_i according to their corresponding eigenvalue λ_i from large to small, therefore, yields a description of the collective motions of the system by the first eigenvectors.

These principal components comply with collective coordinates, including contributions from every atom of the protein, and were shown to make up for the functional dynamics of proteins in several cases [207,210].

3. RESULTS and DISCUSSION

3.1 Equilibration of Lipid Bilayer

Before Pgp simulation the lipid bilayer was prepared and analysed whether or not represent real system. The 512 DMPC (1,2-dimyristoyl-sn-glycero-3-phosphocholine) bilayer was constructed by using 128 pre-equilibrated 128 lipid bilayer. After energy minimization of bilayer, the system was simulated for 1ns and analysed. These analyses are:

- The area per lipid of lipid bilayer was calculated from the lateral x and y dimensions of the simulation box divided by the number of lipid molecules in one leaflet of the bilayer. The Figure 3.1 shows the area per lipid value of prepared lipids. The value of area per lipid was equilibrated about 0.62 and this value is acceptable with compared experimental value of 0.606 [211].
- The deuterium order parameter S_{CD} for the carbon tails is calculated from the elements of the order parameter tensor $S_{xx} = 1/2 \langle (3\cos^2 \alpha_i - 1)/2 \rangle$ and S_{yy} as $S_{CD} = 2/3S_{xx} + 1/3S_{yy}$. The angle α_i is the angle between the molecular axis given by the carbon atoms C_{i-1} and C_{i+1} and the lipid bilayer normal; the average is taken over the time of 0-10 ns and for all lipid molecules. Calculations have been performed with the `g_order` program of the GROMACS suite.

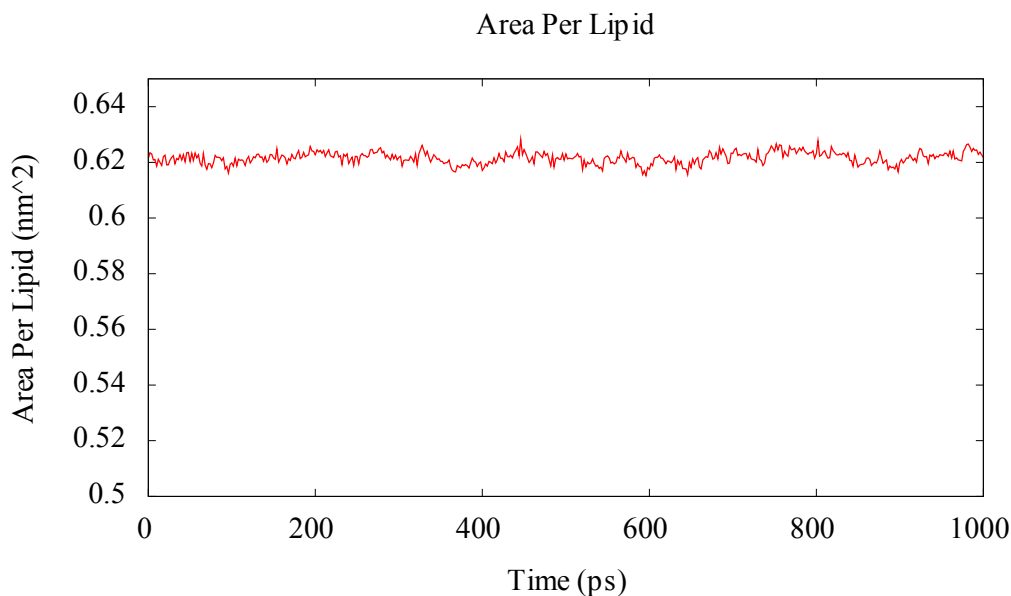


Figure 3.1 : Area per lipid of DMPC. Area per lipid ratio dependent on MD simulation time for a 512-molecule lipid bilayer obtained for DMPC. The experimental value of area per lipid for DMPC is 0.606 [211].

Although the lipid bilayer structure is quite stable, its individual phospholipid and sterol molecules have some freedom of motion. The structure and flexibility of the lipid bilayer depend on temperature and on the lipid types. At relatively low temperatures, the lipids in a bilayer form a semisolid gel phase, in which all types of motion of individual lipid molecules are strongly constrained; the bilayer is paracrystalline. At relatively high temperatures, individual hydrocarbon chains of fatty acids are in constant motion produced by rotation about the carbon-carbon bonds of the long acyl side chains. In this liquid-disordered state, or fluid state, the interior of the bilayer is more fluid than solid and the bilayer is like a sea of constantly moving lipid. At intermediate temperatures, the lipids exist in a liquid-ordered state; there is less thermal motion in the acyl chains of the lipid bilayer, but lateral movement in the plane of the bilayer still takes place. According to Figure 3.2 bilayer the lipids gets into liquid-ordered state and represents in-vivo environment. This lipid bilayer is used for inserting Pgp. After each Pgp simulation these parameters (area per lipid, deuterium order parameters) were checked for stability of lipid bilayer.

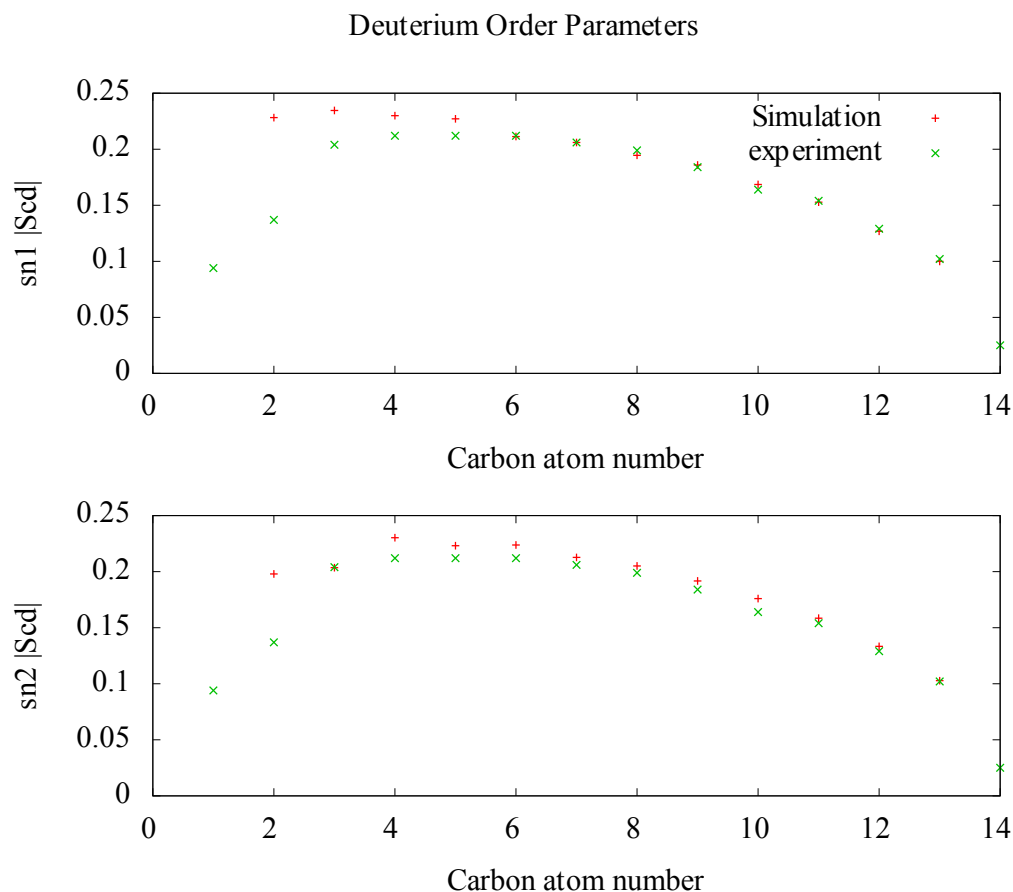


Figure 3.2 : Deuterium order parameters of DMPC bilayer. Comparison of the deuterium order parameters along the carbon atoms of the lipid acyl tails from simulation ($*$) and those from experimental results ($+$). The top plot represents S_{CD} values of sn1 chain and the bottom plot represents S_{CD} values of sn2 chain of lipids. The experimental values are from the sn2 chain in both parts. Experimental deuterium order parameter is taken from [212]. All value is for 310 K(35 C).

3.2 Conformational Stability and Flexibility

The Root Mean Square Deviation (RMSD) of $C\alpha$ atoms with respect to the initial conformation was calculated as a function of time to assess the conformational stability of the protein during the simulations (Figure 3.3).

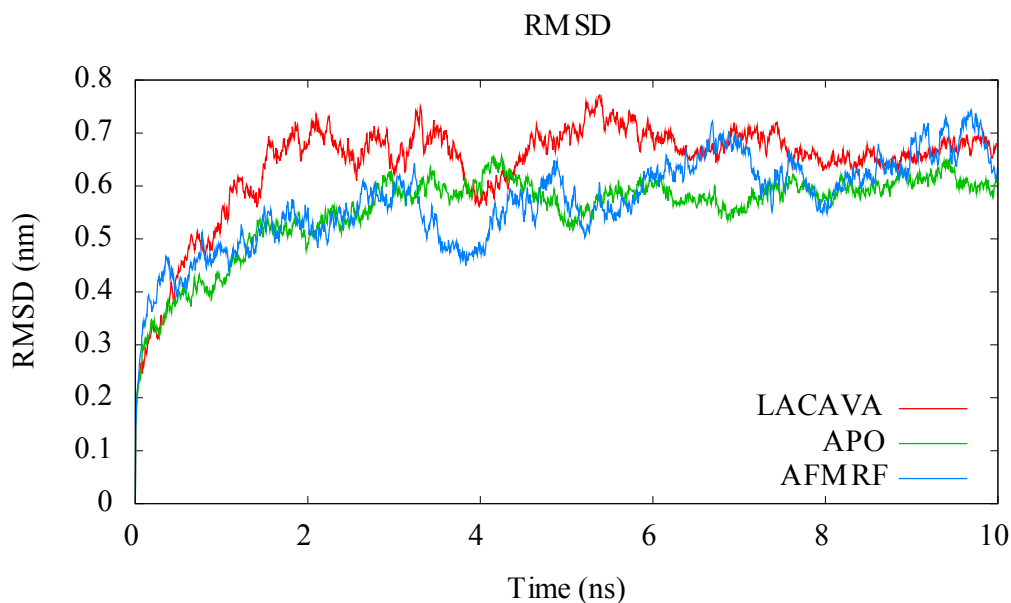


Figure 3.3 : RMSD of simulations. The $C\alpha$ RMSD calculated for the 3 simulation systems. The other simulation results (AFMRF-noATP and ALLM) were not showed.

According to Figure 3.3 APO simulation is equilibrated faster than other two simulations. The reason of this difference is that Pgp with substrate changed its conformation to adopt its substrate. To show this rearrangement in Figure 3.4 the RMSD values of LACAVA simulation presented for each sub domain. We can see easily from this graphic the reason of RMSD fluctuation of LACAVA Simulation is a result of fluctuation with transmembrane domains (TMD). If we extract these fluctuations from RMSD values the simulations were equilibrated around 4 ns.

To identify the flexible regions of the protein, Root Mean Square Fluctuation (RMSF) of $C\alpha$ atoms from its time averaged position was analyzed (Figure 3.5). Generally from APO to LACAVA, RMSF values are increased. Especially the NBD of LACAVA simulation is higher significantly than other simulations. Figure 3.6 shows the b-factor values of LACAVA simulation and the increased fluctuation of NBD can be seen by changing its colour blue into red.

Both RMSD and RMSF analysis give us opinion about convergence of simulation. According to these results and other quality control parameters like minimum distance between periodic images and energy terms (temperature, pressure, potential and kinetics energies) - these parameters are not showed in here - each simulation is quantifiable for further investigations.

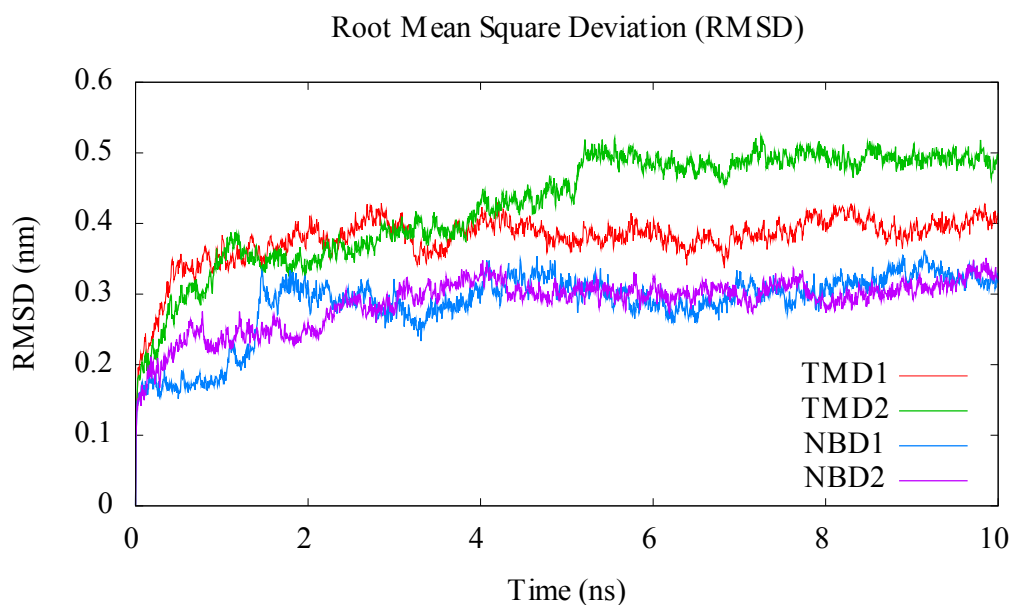


Figure 3.4 : RMSD of LACAVA simulation. This graphic represents RMSD values for each sub domains of Pgp.

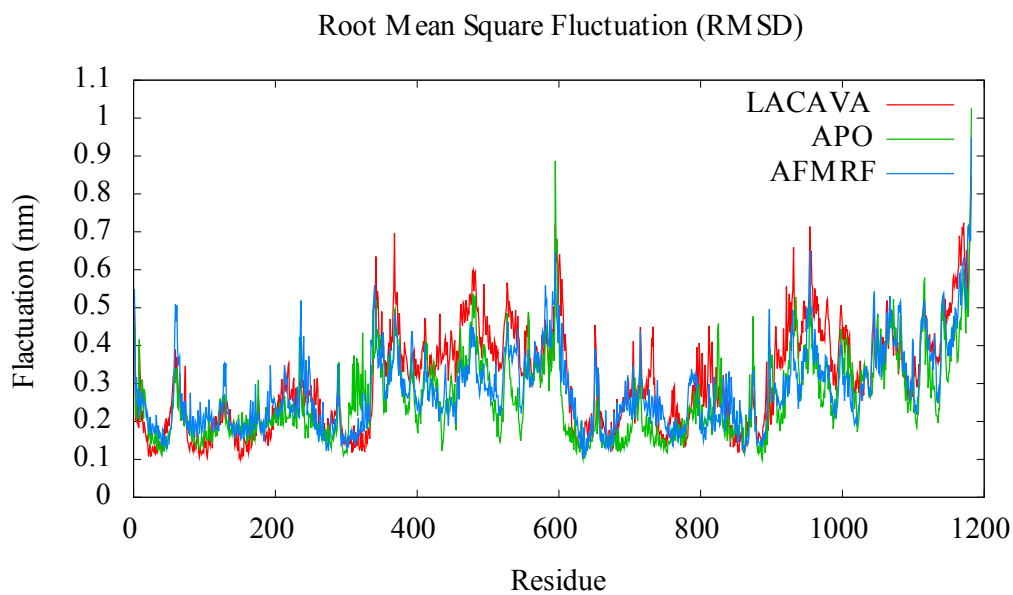


Figure 3.5 : RMSF of simulations. This graph shows RMSF values for each simulation.

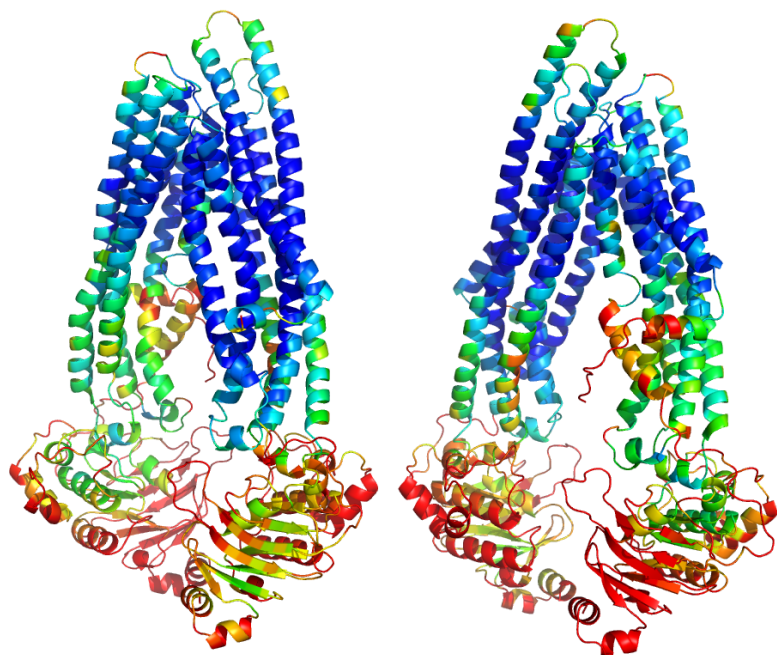


Figure 3.6 : B-factor representation of LACAVA simulation: This figure represents b-factors of Pgp according to LACAVA simulation. From blue to red, the b-factor (fluctuation) values increase. According to this representation ATP binding pocket and lactone atorvastatin pocket has high b-factors. In addition of this high-fluctuated region. Some intra-domain regions has high b-factors like binding pockets.

3.3 Principal Component Analysis (PCA)

The prominent motions in the transporter during the course of simulation were analyzed with the help of PCA [207]. The principal motions for first eigenvectors of the three simulations are visualized using porcupine plot (see Figure 3.7). First eigenvector account for 40%, 37% and 76% of the motions in apo, AFMRF peptide and atorvastatin lactone bound simulations, respectively.

We observed a concerted movement of TM helices within domains TMD1 and TMD2 during the simulations, suggesting a rigid body movement of these domains. The noticeable motion in the apo form simulation was a opening of the two transmembrane domains relative to one another, and is shown as a schematic diagram in Figure 3.7 APO. While in the case of atorvastatin lactone bound form (see Figure 3.7 LACAVA), domains showed an closing motion type movement and TM4-5 and TM10-11 has a twisting motion in addition to closure. However, the molecular dynamics of AFMRF bound form of the transporter (see Figure 3.7

AFMRF) has a closing motion but its motion degree is lower than atorvastatin lactone bond form.

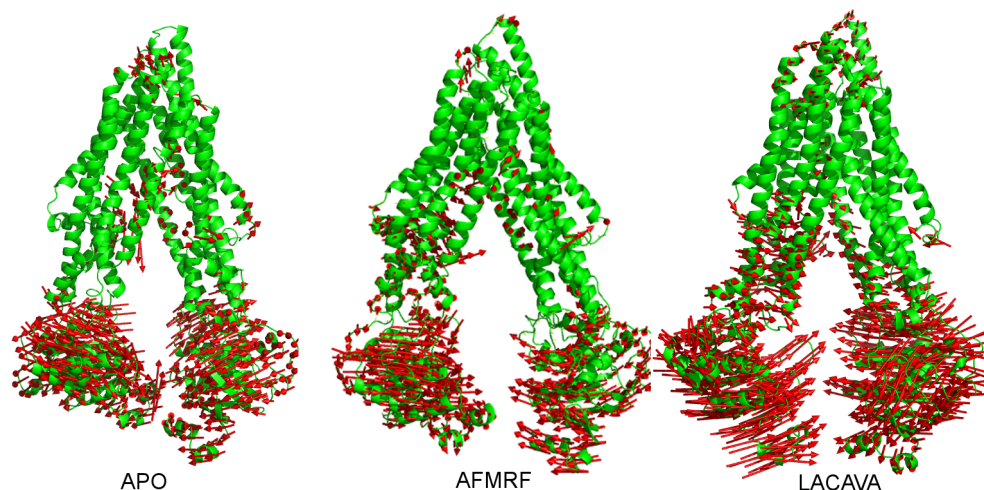


Figure 3.7 : PCA of Pgp simulations. The principal motions for first eigen vectors of the three simulations are represented in this figure. The direction of red arrows shows the direction of motion and the length of arrows shows the magnitude of motion.

Proteins often accomplish their functions through collective atomic motions. To examine which residues undergo concerted motions, we analyzed the covariance matrix (see Figure 3.8) derived from the sets of conformations generated in the 10 ns simulations. This analysis highlighted regions of the protein that move together. The NBD1 (350-600) and NBD2 (residue 850-1200) has intensive correlations with the opposite direction. Aside from anticipated correlations between NBD we can see that some transmembrane domains have correlations and moves with NBD domain. TM4-5 and TM10-11 were found to correlate with each other.

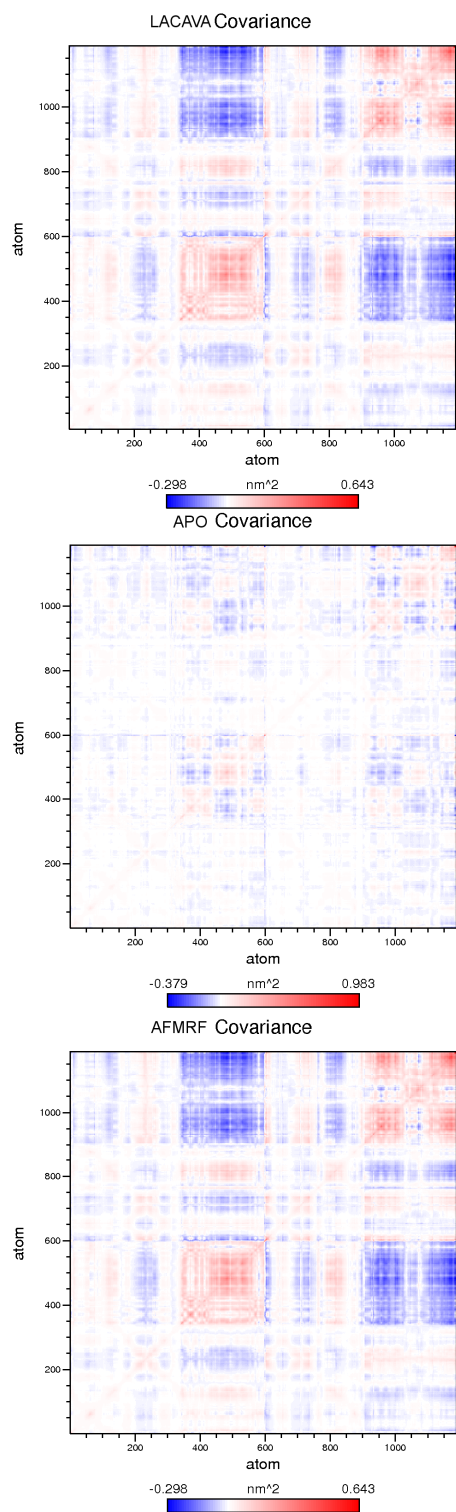


Figure 3.8 : Covariance matrix of simulations. The matrix shows the covariance between atoms. Red means that two atoms move together, whereas blue means they move opposite to each other. The intensity of the red color is indicating the amplitude of the fluctuations.

3.4 Inter-helical Hydrogen Bonds

Hydrogen bonds formed between TM helices are shown to play a critical role in stabilizing the tertiary structure of membrane proteins as well as in the conformational rearrangement required for specific functions [213]. We analyzed all possible inter-helical hydrogen bonds formed by Pgp during the time period of molecular dynamics simulation. Several inter and intra-domain hydrogen bonds were identified, and significant rearrangements of the hydrogen bonds were also observed in the three simulation systems. For LACAVA simulation, TM10-11, TM2-11 and TM9-7 interact with its counterpart through an increased hydrogen bonding (See Figure 3.9). TM9-7 interactions has special role its hydrogen bonding significantly increased when any substrate binded to Pgp. With LACAVA simulation TM1-2 hydrogen bonding is higher than AFMRF and ALLM peptide bond form.

To see big picture of hydrogen bonding profile it is possible to look only interdomain hydrogen bonding. Figure 3.10 shows that inter-transmembrane and inter-nucleotide binding domain interactions increased during simulation. Especially for TMDs and NBDs, inter-domain hydrogen bonding is increased during simulation and this increased hydrogen bonding stabilizes the closure of Pgp for LACAVA simulation.

Inter Helical Hydrogen Bonding

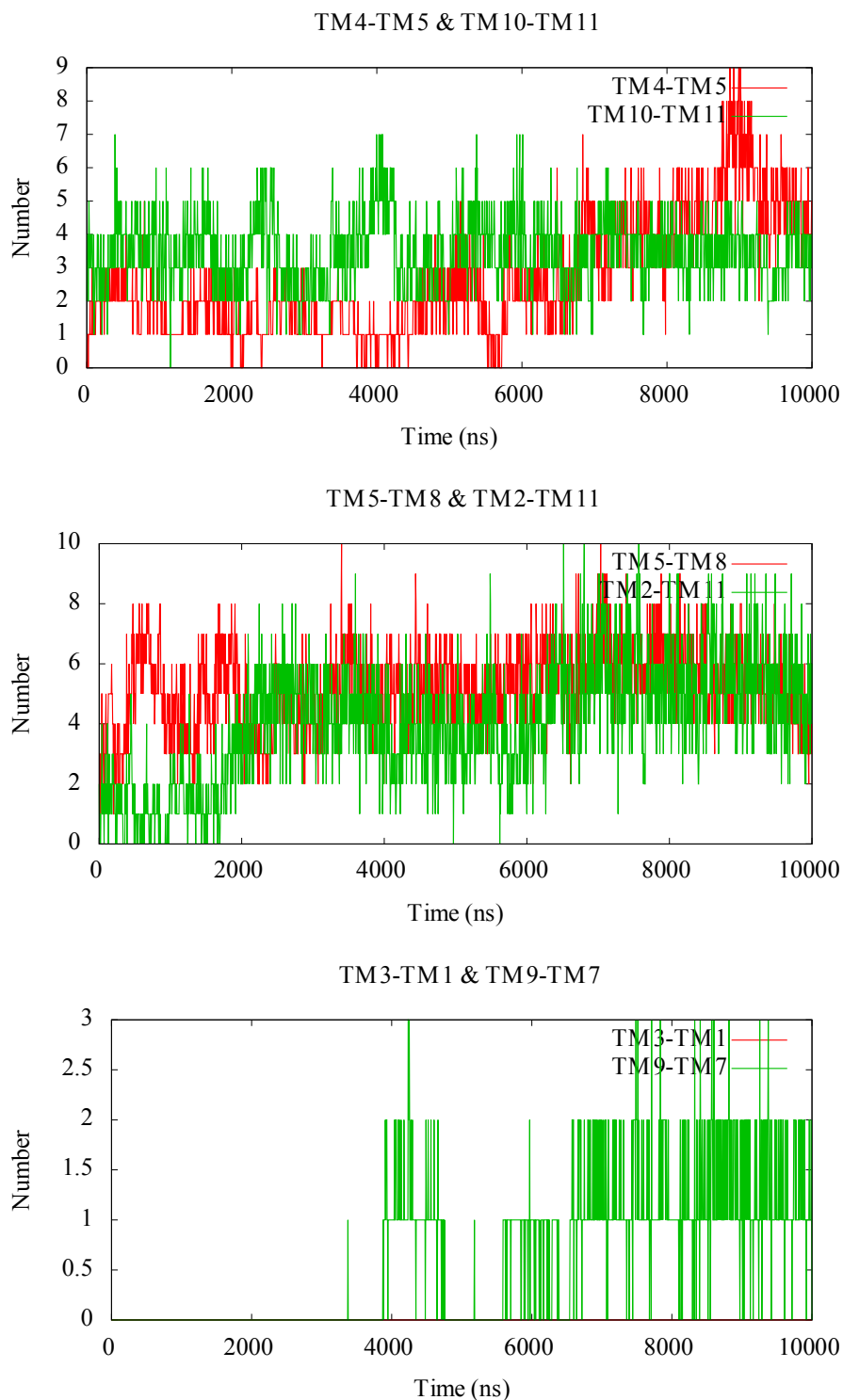
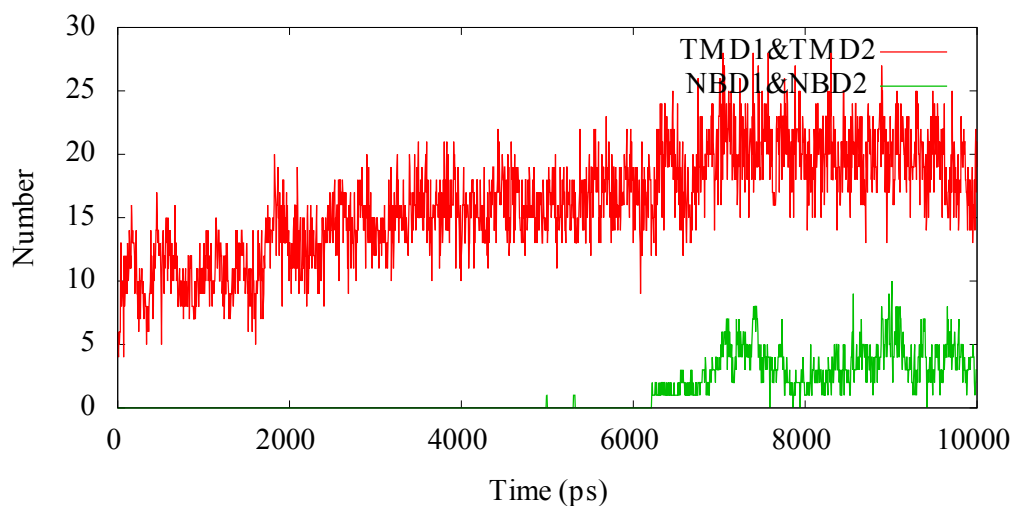


Figure 3.9 : LACAVA inter-helical hydrogen bonding. The hydrogen bonding number of LACAVA simulation for TM10-11, TM1-11 and TM9-7. The bonding profiles give opinion which transmembrane helices have more roles during transporting.

Hydrogen Bonding

TMD1-TMD2 & NBD1-NBD2



TMD1-NBD1 & TMD2-NBD2

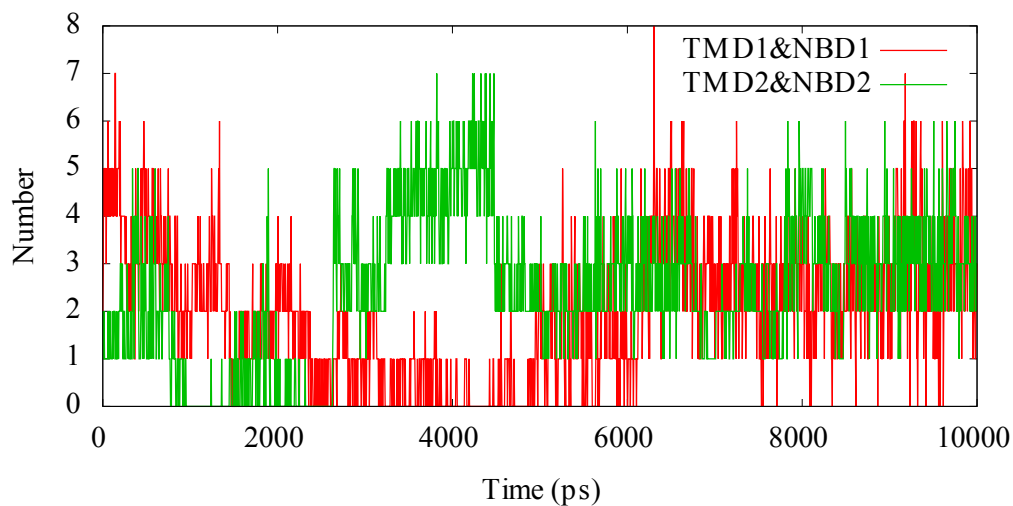


Figure 3.10 : Interdomain Hydrogen Bonding Profile. This plot show how the numbers of hydrogen bond between domains change during LACAVA simulation. According to this figure, the number of hydrogen bonding between TMD1-TMD2 and NBD1-NBD2 increased. However, the hydrogen bonding profile between TMD and NBD fluctuated and after for while this fluctuation is equilibrated.

3.5 ATP Binding

The catalytic cycle of Pgp involves the coupling of ATP binding and hydrolysis with substrate translocation across the cell membrane. Reactions taking place at the NBDs

during the catalytic cycle include ATP binding and formation of a nucleotide sandwich dimer, followed by ATP hydrolysis, P_i dissociation, and finally ADP dissociation. The simulation result of LACAVA simulation has asymmetric closure for ATP binding pocket. Although the simulation duration was short we could see the starting closure for one of the binding pocket of LACAVA system (see Figure 3.13). The other APO (see Figure 3.11) and AFMRF (see Figure 3.12) simulations have no remarkable closure for ATP binding pocket.

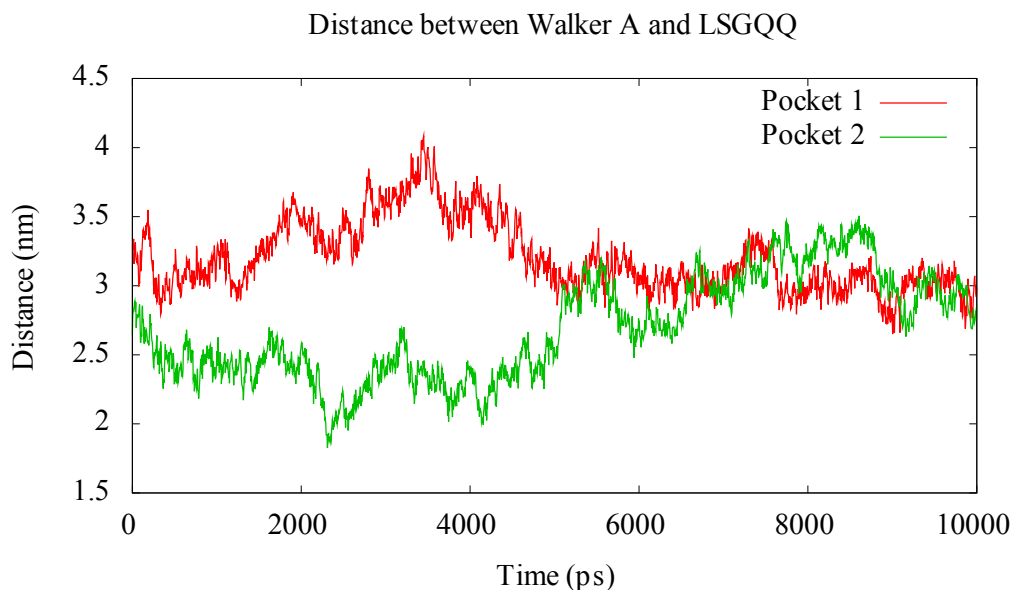


Figure 3.11 : Distance between Walker A and LSGGQ for APO simulation. This plot show how distance between Walker A and LSGGQ signature motif changed during simulation. According to this plot after a fluctuation, the distances for each pocket are equilibrated. Any closure motion for NBDs was not seen.

The simulation results show that only for LACAVA simulation has a closure motion for one of its ATP binding pocket. And this closure motion is asymmetric closure as defined previous studies [120]. A few simulation studies which were done for Sav1866 MDR protein [214,215] concluded same result with this LACAVA simulation. As discussed previously in introduction section the asymmetric ATP hydrolyses is suggested [120] for MDR proteins. And the LACAVA result is matching to this mechanism. But the duration of simulation is not enough to be sure whether or not the asymmetric closure for LACAVA is final conformation of this simulation. Because this conformation can be results of random starting conditions and can leave this conformation with longer simulation.

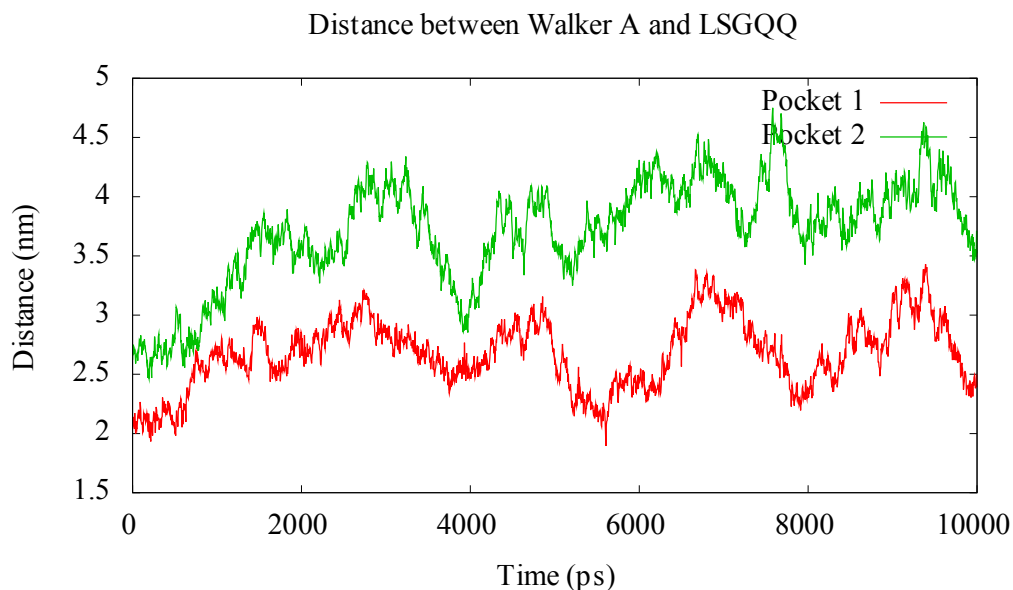


Figure 3.12 : Distance between Walker A and LSGGQ for AFMRF simulation: This plot show how distance between Walker A and LSGGQ signature motif changed during simulation. According to this plot there, the fluctuation of distance value was not equilibrated and any closure for ATP binding pocket was not seen.

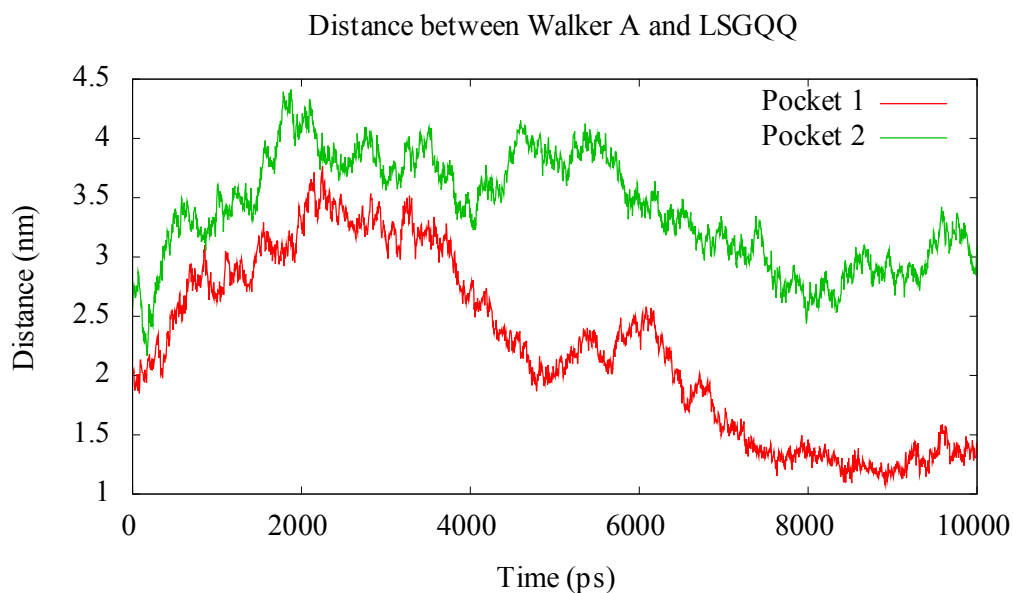


Figure 3.13 : Distance between Walker A and LSGGQ for LACAVA simulation. This plot show how distance between Walker A and LSGGQ signature motif changed during simulation. According to this plot, we can see that there is a closure in one of the ATP binding pockets. The other ATP binding pocket not closing one was fluctuated during simulation.

4. CONCLUSION

P-Glycoprotein is a drug transporter of the ABC superfamily that functions as an ATP-powered drug efflux pump. Rapid progress has been made in recent years in understanding the three-dimensional structure and ATP hydrolysis cycle of this protein, and many tools are now available for its study at the molecular level. Although the transporter can interact with hundreds of nonpolar, weakly amphipathic compounds with no apparent structural similarity, progress is being made in developing a pharmacophore model to describe its binding regions. The protein appears to interact with its multiple substrates via a large flexible drug-binding pocket, to which drugs gain access from the bilayer, leading to the suggestion that it is a “vacuum cleaner” for hydrophobic compounds that concentrate within the membrane. The drug transport mechanism of Pgp is poorly described and may involve “flipping” of substrates from the inner to the outer membrane leaflet. The primary physiological role of the protein appears to be the protection of sensitive organs and tissues from xenobiotic toxicity. Many drugs used in clinical therapy are P-glycoprotein substrates, and the transporter is now increasingly recognized to play a central role in the absorption and disposition of many drugs, including chemotherapeutic agents. Other compounds, known as modulators, that block the drug efflux function of Pgp are under development and may have clinical applications in the future.

With release of crystal structure of Pgp, molecular dynamic simulation can create great opportunities to discover Pgp mechanism. If we resolve the mechanism of Pgp we can increasingly rationalize the drug development process of disease like cancer. Molecular dynamics simulation gives us to investigate atomistic level mechanism.

This study investigated Pgp mechanism with some linear peptides and lactone atorvastatin. Because of low resolution of structure of Pgp there is some problem to investigate structure. Although this obstacle about structure we can say that Pgp interacted with lactone form of atorvastatin and has asymmetrical closure of nucleotide binding domains as we see with other MDR proteins like Sav1866.

In spite of atorvastatin interaction with Pgp, any meaningful interactions with linear peptides were not seen from simulation results. These peptides were selected because both ALLM (N-acetyl-leu-leu-met-al) and AFMRF (N-acetyl-phe-met-phe-arg-phe-al) are characterized as a substrates of Pgp and topology preparation was not required. There are some possible reasons for non-interactions between peptides and Pgp. One of these reasons can be that single peptide was not enough to interact with Pgp. Because we have known that Pgp has large polyspecific drug binding pocket and can transport more than one molecule per transport cycle.

Ideas for further studies arising from the results of this work are manifold. First, simulations of lactone atorvastatin should be continued to further understand the mechanism of Pgp and which residues are critic for transportation and to develop ways to better combine simulations with experiments. Also, work on acid form of atorvastatin should be investigated to understand which form of atorvastatin interacts with Pgp. In addition to atorvastatin, other statin molecules should be included in simulation to understand the drug metabolism of statins.

REFERENCES

- [1] **Biedler, J. and Riehm, H.**, 1970. Cellular resistance to actinomycin D in Chinese hamster cells *in vitro*: cross-resistance, radioautographic, and cytogenetic studies, *Cancer Res.*, **30**, 1174–1184.
- [2] **Riordan, J. and Ling, V.**, 1985. Genetic and biochemical characterization of multidrug resistance, *Pharmacology & therapeutics*, **28**, 51–75.
- [3] **Shen, D., Cardarelli, C., Hwang, J., Cornwell, M., Richert, N., Ishii, S., Pastan, I. and Gottesman, M.**, 1986. Multiple drug-resistant human KB carcinoma cells independently selected for high-level resistance to colchicine, adriamycin, or vinblastine show changes in expression of specific proteins., *Journal of Biological Chemistry*, **261**, 7762.
- [4] **Ling, V. and Thompson, L.**, 1974. Reduced permeability in CHO cells as a mechanism of resistance to colchicine, *Journal of Cellular Physiology*, **83**.
- [5] **See, Y., Carlsen, S., Till, J. and Ling, V.**, 1974. Increased drug permeability in Chinese hamster ovary cells in the presence of cyanide, *Biochimica et Biophysica Acta (BBA)-Biomembranes*, **373**, 242–252.
- [6] **Juliano, R. and Ling, V.**, 1976. A surface glycoprotein modulating drug permeability in Chinese hamster ovary cell mutants, *Biochim Biophys Acta*, **455**, 152–162.
- [7] **Gerlach, J., Endicott, J., Juranka, P., Henderson, G., Sarangi, F., Deuchars, K. and Ling, V.**, 1986. Homology between P-glycoprotein and a bacterial haemolysin transport protein suggests a model for multidrug resistance, *Nature*, **324**, 485–489.
- [8] **Chen, C., Chin, J., Ueda, K., Clark, D., Pastan, I., Gottesman, M. and Roninson, I.**, 1986. Internal duplication and homology with bacterial transport proteins in the *mdr1* (P-glycoprotein) gene from multidrug-resistant human cells, *Cell*, **47**, 381–389.
- [9] **Gros, P., Ben, N., Croop, J. and Housman, D.**, 1986. Isolation and expression of a complementary DNA that confers multidrug resistance, *Nature*, **323**, 728–731.
- [10] **Gottesman, M. and Pastan, I.**, 1993. Biochemistry of multidrug resistance mediated by the multidrug transporter, *Annu. Rev. Biochem.*, **62**, 385–427.
- [11] **Jones, P. and George, A.**, 2004. The ABC transporter structure and mechanism: perspectives on recent research, *Cellular and Molecular Life Sciences*, **61**, 682–699.

- [12] **Dean, D., Davidson, A. and Nikaido, H.**, 1989. Maltose transport in membrane vesicles of *Escherichia coli* is linked to ATP hydrolysis, *Proceedings of the National Academy of Sciences*, **86**, 9134–9138.
- [13] **Ames, G., Nikaido, K., Groarke, J. and Petithory, J.**, 1989. Reconstitution of periplasmic transport in inside-out membrane vesicles. Energization by ATP, *Journal of Biological Chemistry*, **264**, 3998–4002.
- [14] **Davidson, A., Dassa, E., Orelle, C. and Chen, J.**, 2008. Structure, function, and evolution of bacterial ATP-binding cassette systems, *Microbiol. Mol. Biol. Rev.*, **72**, 317–364.
- [15] **Hollenstein, K., Frei, D.C. and Locher, K.P.A.**, 2007. Structure of an ABC transporter in complex with its binding protein, *Nature*, **446**, 213–216.
- [16] **Aller, S.G., Yu, J., Ward, A., Weng, Y., Chittaboina, S., Zhuo, R., Harrell, P.M., Trinh, Y.T., Zhang, Q., Urbatsch, I.L. and Chang, G.**, 2009. Structure of P-Glycoprotein Reveals a Molecular Basis for Poly-Specific Drug Binding, *Science*, **323**, 1718 – 1722.
- [17] **Dawson, R.J. and Locher, K.P.**, 2006. Structure of a bacterial multidrug ABC transporter, *Nature*, **443**, 180–185.
- [18] **Linton, K.J. and Higgins, C.F.**, 1998. The *Escherichia coli* ATP-binding cassette (ABC) proteins, *Mol. Microbiol.*, **28**, 5–13.
- [19] **Dean, M., Rzhetsky, A. and Allikmets, R.**, 2001. The human ATP-binding cassette (ABC) transporter superfamily, *Annu. Rev. Cell Biol.*, **11**, 1156–1166.
- [20] **Gottesman, M.M. and Ambudkar, S.V.**, 2001. Overview: ABC transporters and human disease, *J. Bioenerg. Biomembr.*, **33**, 453–458.
- [21] **Biemans-Oldehinkel, E., Doeven, M.K. and Poolman, B.**, 2006. ABC transporter architecture and regulatory roles of accessory domains, *FEBS Letters*, **580**, 1023–1035.
- [22] **Ames, G.F.L.**, 1986. Bacterial periplasmic transport systems structure, mechanism and evolution, *Annu. Rev. Biochem.*, **55**, 397–425.
- [23] **Hollenstein, K., Dawson, R.J.P. and Locher, K.P.**, 2007. Structure and mechanism of ABC transporter proteins, *Current Opinion in Structural Biology*, **17**, 412–418.
- [24] **Thiebaut, F., Tsuruo, T., Hamada, H., Gottesman, M., Pastan, I. and Willingham, M.**, 1987. Cellular localization of the multidrug-resistance gene product P-glycoprotein in normal human tissues, *Proceedings of the National Academy of Sciences of the United States of America*, **84**, 7735.
- [25] **Croop, J., Raymond, M., Haber, D., Devault, A., Arceci, R., Gros, P. and Housman, D.**, 1989. The three mouse multidrug resistance (mdr) genes are expressed in a tissue-specific manner in normal mouse tissues., *Molecular and cellular biology*, **9**, 1346.
- [26] **Beaulieu, E., Demeule, M., Ghitescu, L. and Beliveau, R.**, 1997. P-glycoprotein is strongly expressed in the luminal membranes of the

- endothelium of blood vessels in the brain., *Biochemical Journal*, **326**, 539.
- [27] **Melaine, N., Liénard, M., Dorval, I., Le Goascogne, C., Lejeune, H. and Jégou, B.**, 2002. Multidrug resistance genes and p-glycoprotein in the testis of the rat, mouse, Guinea pig, and human, *Biology of reproduction*, **67**, 1699.
- [28] **Edwards, J., Alcorn, J., Savolainen, J., Anderson, B. and McNamara, P.**, 2005. Role of P-glycoprotein in distribution of nelfinavir across the blood-mammary tissue barrier and blood-brain barrier, *Antimicrobial agents and chemotherapy*, **49**, 1626.
- [29] **Saito, T., Zhang, Z., Tsuzuki, H., Ohtsubo, T., Yamada, T., Yamamoto, T. and Saito, H.**, 1997. Expression of P-glycoprotein in inner ear capillary endothelial cells of the guinea pig with special reference to blood-inner ear barrier, *Brain research*, **767**, 388–392.
- [30] **Arceci, R., Croop, J., Horwitz, S. and Housman, D.**, 1988. The gene encoding multidrug resistance is induced and expressed at high levels during pregnancy in the secretory epithelium of the uterus, *Proceedings of the National Academy of Sciences of the United States of America*, **85**, 4350.
- [31] **Gil, S., Saura, R., Forestier, F. and Farinotti, R.**, 2005. P-glycoprotein expression of the human placenta during pregnancy, *Placenta*, **26**, 268–270.
- [32] **Kalabis, G., Kostaki, A., Andrews, M., Petropoulos, S., Gibb, W. and Matthews, S.**, 2005. Multidrug resistance phosphoglycoprotein (ABCB1) in the mouse placenta: fetal protection, *Biology of reproduction*, **73**, 591.
- [33] **Smit, J., Schinkel, A., Mol, C., Majoor, D., Mooi, W., Jongsma, A., Lincke, C. and Borst, P.**, 1994. Tissue distribution of the human MDR3 P-glycoprotein., *Laboratory investigation; a journal of technical methods and pathology*, **71**, 638.
- [34] **Schinkel, A.**, 1998. Pharmacological insights from P-glycoprotein knockout mice., *International journal of clinical pharmacology and therapeutics*, **36**, 9.
- [35] **Schinkel, A., Smit, J., Van Tellingen, O., Beijnen, J., Wagenaar, E., Van Deemter, L., Mol, C., Van der Valk, M., Robanus-Maandag, E. and Te Riele, H.**, 1994. Disruption of the mouse mdr1a P-glycoprotein gene leads to a deficiency in the blood-brain barrier and to increased sensitivity to drugs, *Cell*, **77**, 491–502.
- [36] **Jette, L., Pouliot, J., Murphy, G. and Beliveau, R.**, 1995. Isoform I (mdr3) is the major form of P-glycoprotein expressed in mouse brain capillaries. Evidence for cross-reactivity of antibody C219 with an unrelated protein., *Biochemical Journal*, **305**, 761.

- [37] **Doran, A., Obach, R., Smith, B., Hosea, N., Becker, S., Callegari, E., Chen, C., Chen, X., Choo, E. and Cianfrogna, J.**, 2005. The impact of P-glycoprotein on the disposition of drugs targeted for indications of the central nervous system: evaluation using the MDR1A/1B knockout mouse model, *Science's STKE*, **33**, 165.
- [38] **Roulet, A., Puel, O., Gesta, S., Lepage, J., Drag, M., Soll, M., Alvinerie, M. and Pineau, T.**, 2003. MDR1-deficient genotype in Collie dogs hypersensitive to the P-glycoprotein substrate ivermectin* 1, *European Journal of Pharmacology*, **460**, 85–91.
- [39] **Nelson, O., Carsten, E., Bentjen, S. and Mealey, K.**, 2003. Ivermectin toxicity in an Australian Shepherd dog with the MDR1 mutation associated with ivermectin sensitivity in Collies, *Journal of veterinary internal medicine*, **17**, 354–356.
- [40] **Neff, M., Robertson, K., Wong, A., Safra, N., Broman, K., Slatkin, M., Mealey, K. and Pedersen, N.**, 2004. Breed distribution and history of canine *mdr1-1Δ*, a pharmacogenetic mutation that marks the emergence of breeds from the collie lineage, *Proceedings of the National Academy of Sciences of the United States of America*, **101**, 11725.
- [41] **Gottesman, M.M., Fojo, T. and Bates, S.E.**, 2001. Multidrug resistance in cancer role of ATP-dependent transporters, *Nature Rev. Cancer*, **2**, 48–58.
- [42] **Goldstein, L., Galski, H., Fojo, A., Willingham, M., Lai, S., Gazdar, A., Pirker, R., Green, A., Crist, W. and Brodeur, G.**, 1989. Expression of a multidrug resistance gene in human cancers, *J. Natl. Cancer Inst.*, **81**, 116–124.
- [43] **Sorrentino, B., Brandt, S., Bodine, D., Gottesman, M., Pastan, I., Cline, A. and Nienhuis, A.**, 1992. Selection of drug-resistant bone marrow cells *in vivo* after retroviral transfer of human MDR1, *Science*, **257**, 99.
- [44] **Sasongko, L., Link, J., Muzi, M., Mankoff, D., Yang, X., Collier, A., Shoner, S. and Unadkat, J.**, 2005. Imaging P-glycoprotein Transport Activity at the Human Blood-brain Barrier with Positron Emission Tomographyast, *Clinical Pharmacology and Therapeutics*, **77**, 503–514.
- [45] **Robert, J. and Jarry, C.**, 2003. Multidrug resistance reversal agents, *J. Med. Chem.*, **46**, 4805–4817.
- [46] **Dayan, G., Jault, J., Baubichon-Cortay, H., Baggetto, L., Renoir, J., Baulieu, E., Gros, P. and Di Pietro, A.**, 1997. Binding of Steroid Modulators to Recombinant Cytosolic Domain from Mouse P-Glycoprotein in Close Proximity to the ATP Site, *Biochemistry*, **36**, 15208–15215.
- [47] **List, A., Kopecky, K., Willman, C., Head, D., Persons, D., Slovak, M., Dorr, R., Karanes, C., Hynes, H. and Doroshow, J.**, 2001. Benefit of cyclosporine modulation of drug resistance in patients with poor-risk acute myeloid leukemia: a Southwest Oncology Group study, *Blood*, **98**, 3212.

- [48] **Polgar, O. and Bates, S.**, 2005. ABC transporters in the balance: is there a role in multidrug resistance? , *Biochemical Society Transactions*, **33**, 241–245.
- [49] **Aszalos, A.**, 2007. Drug-drug interactions affected by the transporter protein, P-glycoprotein (ABCB1, MDR1):: II. Clinical aspects, *Drug discovery today*, **12**, 838–843.
- [50] **Schinkel, A.**, 1999. P-Glycoprotein, a gatekeeper in the blood-brain barrier, *Advanced drug delivery reviews*, **36**, 179–194.
- [51] **Krahenbuhl, S., Menafoglio, A., Giostra, E. and Gallino, A.**, 1998. Serious Interaction Between Mibefradil and Tacrolimus1, *Transplantation*, **66**, 1113.
- [52] **Greiner, B., Eichelbaum, M., Fritz, P., Kreichgauer, H., Von Richter, O., Zundler, J. and Kroemer, H.**, 1999. The role of intestinal P-glycoprotein in the interaction of digoxin and rifampin, *Journal of Clinical Investigation*, **104**, 147–153.
- [53] **Durr, D., Stieger, B., Kullak-Ublick, G., Rentsch, K., Steinert, H., Meier, P. and Fattinger, K.**, 2000. St John's Wort induces intestinal P-glycoprotein/MDR1 and intestinal and hepatic CYP3A4, *Clinical Pharmacology and Therapeutics*, **68**, 598–604.
- [54] **Giacomini, K., Huang, S., Tweedie, D., Benet, L., Brouwer, K., Chu, X., Dahlin, A., Evers, R., Fischer, V. and Hillgren, K.**, 2010. Membrane transporters in drug development, *Nature Reviews Drug Discovery*, **9**, 215–236.
- [55] **Szakacs, G., Paterson, J., Ludwig, J., Booth-Genthe, C. and Gottesman, M.**, 2006. Targeting multidrug resistance in cancer, *Nature Reviews Drug Discovery*, **5**, 219–234.
- [56] **Szakacs, G., Annereau, J., Lababidi, S., Shankavaram, U., Arciello, A., Bussey, K., Reinhold, W., Guo, Y., Kruh, G. and Reimers, M.**, 2004. Predicting drug sensitivity and resistance:: Profiling ABC transporter genes in cancer cells, *Cancer Cell*, **6**, 129–137.
- [57] **Ludwig, J., Szakacs, G., Martin, S., Chu, B., Cardarelli, C., Sauna, Z., Caplen, N., Fales, H., Ambudkar, S. and Weinstein, J.**, 2006. Selective toxicity of NSC73306 in MDR1-positive cells as a new strategy to circumvent multidrug resistance in cancer, *Cancer research*, **66**, 4808.
- [58] **Leschziner, G., Andrew, T., Pirmohamed, M. and Johnson, M.**, 2006. ABCB1 genotype and PGP expression, function and therapeutic drug response: a critical review and recommendations for future research, *The pharmacogenomics journal*, **7**, 154–179.
- [59] **Kimchi-Sarfaty, C., Oh, J., Kim, I., Sauna, Z., Calcagno, A., Ambudkar, S. and Gottesman, M.**, 2007. A " silent" polymorphism in the MDR1 gene changes substrate specificity, *Science*, **315**, 525.
- [60] **Kast, C., Canfield, V., Levenson, R. and Gros, P.**, 1996. Transmembrane organization of mouse P-glycoprotein determined by epitope insertion and immunofluorescence, *Journal of Biological Chemistry*, **271**, 9240.

- [61] **Loo, T. and Clarke, D.**, 1995. Membrane topology of a cysteine-less mutant of human P-glycoprotein, *Journal of Biological Chemistry*, **270**, 843.
- [62] **Higgins, C.F.**, 1992. ABC transporters from microorganisms to man, *Annu. Rev. Cell Biol.*, **8**, 67–113.
- [63] **Rosenberg, M.F., Callaghan, R., Ford, R.C. and Higgins, C.F.**, 1997. Structure of the multidrug resistance P-glycoprotein to 2.5 nm resolution determined by electron microscopy and image analysis, *The Journal Of Biological Chemistry*, **272**, 10685–10694.
- [64] **Rosenberg, M., Velarde, G., Ford, R., Martin, C., Berridge, G., Kerr, I., Callaghan, R., Schmidlin, A., Wooding, C. and Linton, K.**, 2001. Repacking of the transmembrane domains of P-glycoprotein during the transport ATPase cycle, *The EMBO Journal*, **20**, 5615.
- [65] **Rosenberg, M.F., Kamis, A.B., Callaghan, R., Higgins, C.F. and Ford, R.C.**, 2003. Three-dimensional Structures of the Mammalian Multidrug Resistance P-glycoprotein Demonstrate Major Conformational Changes in the Transmembrane Domains upon Nucleotide Binding, *The Journal Of Biological Chemistry*, **278**, 8294–8299.
- [66] **Rosenberg, M.F., Callaghan, R., Modok, S., Higgins, C.F. and Ford, R.C.**, 2005. Three-dimensional structure of P-glycoprotein: the transmembrane regions adopt an asymmetric configuration in the nucleotide-bound state, *The Journal Of Biological Chemistry*, **280**, 2857–2862.
- [67] **Dawson, R.J. and Locher, K.P.**, 2007. Structure of the multidrug ABC transporter Sav1866 from *Staphylococcus aureus* in complex with AMP-PNP, *FEBS Letters*, **581**, 935–938.
- [68] **Loo, T. and Clarke, D.**, 2000. The packing of the transmembrane segments of human multidrug resistance P-glycoprotein is revealed by disulfide cross-linking analysis, *Journal of Biological Chemistry*, **275**, 5253.
- [69] **Loo, T.W. and Clarke, D.M.**, 1997. Identification of Residues in the Drug-binding Site of Human P-glycoprotein Using a Thiol-reactive Substrate, *The Journal Of Biological Chemistry*, **272**, 31945–31948.
- [70] **Loo, T. and Clarke, D.**, 1999. Merck Frosst Award Lecture 1998. Molecular dissection of the human multidrug resistance P-glycoprotein., *Biochemistry and cell biology= Biochimie et biologie cellulaire*, **77**, 11.
- [71] **Loo, T. and Clarke, D.**, 1999. Identification of residues in the drug-binding domain of human P-glycoprotein. Analysis of transmembrane segment 11 by cysteine-scanning mutagenesis and inhibition by dibromobimane., *The Journal of biological chemistry*, **274**, 35388.
- [72] **Loo, T. and Clarke, D.**, 2000. Identification of residues within the drug-binding domain of the human multidrug resistance P-glycoprotein by cysteine-scanning mutagenesis and reaction with dibromobimane, *Journal of Biological Chemistry*, **275**, 39272.

- [73] **Loo, T. and Clarke, D.**, 2005. Recent progress in understanding the mechanism of P-glycoprotein-mediated drug efflux, *Journal of Membrane Biology*, **206**, 173–185.
- [74] **Qu, Q. and Sharom, F.**, 2001. FRET Analysis Indicates That the Two ATPase Active Sites of the P-Glycoprotein Multidrug Transporter Are Closely Associated, *Biochemistry*, **40**, 1413–1422.
- [75] **Liu, R. and Sharom, F.**, 1998. Proximity of the Nucleotide Binding Domains of the P-glycoprotein Multidrug Transporter to the Membrane Surface: A Resonance Energy Transfer Study, *Biochemistry*, **37**, 6503–6512.
- [76] **Qu, Q. and Sharom, F.**, 2002. Proximity of Bound Hoechst 33342 to the ATPase Catalytic Sites Places the Drug Binding Site of P-glycoprotein within the Cytoplasmic Membrane Leaflet, *Biochemistry*, **41**, 4744–4752.
- [77] **Lugo, M. and Sharom, F.**, 2005. Interaction of LDS-751 with P-Glycoprotein and Mapping of the Location of the R Drug Binding Site, *Biochemistry*, **44**, 643–655.
- [78] **Zolnerciks, J.K., Wooding, C. and Linton, K.J.**, 2007. Evidence for a Sav1866-like architecture for the human multidrug transporter P-glycoprotein, *FEBS Letters*, **21**, 3937–3948.
- [79] **Eckford, P. and Sharom, F.**, 2009. ABC efflux pump-based resistance to chemotherapy drugs, *Chemical Reviews*, **109**, 2989–3011.
- [80] **Ward, A., Reyes, C.L., Yu, J., Roth, C.B. and Chang, G.**, 2007. Flexibility in the ABC transporter MsbA: alternating access with a twist, *PNAS*, **104**, 19005–19010.
- [81] **Dawson, R.J.P., Hollenstein, K. and Locher, K.P.**, 2007. Uptake or extrusion: crystal structures of full ABC transporters suggest a common mechanism, *Molecular Microbiology*, **65**, 250–257.
- [82] **Haubertin, D., Madaoui, H., Sanson, A., Guerois, R. and Orłowski, S.**, 2006. Molecular dynamics simulations of *E. coli* MsbA transmembrane domain: formation of a semipore structure, *Biophysical journal*, **91**, 2517–2531.
- [83] **Dong, J., Yang, G. and Mchaourab, H.**, 2005. Structural basis of energy transduction in the transport cycle of MsbA, *Science*, **308**, 1023–1028.
- [84] **Buchaklian, A., Funk, A. and Klug, C.**, 2004. Resting state conformation of the MsbA homodimer as studied by site-directed spin labeling, *Biochemistry*, **43**, 8600–8606.
- [85] **Hrycyna, C., Airan, L., Germann, U., Ambudkar, S., Pastan, I. and Gottesman, M.**, 1998. Structural Flexibility of the Linker Region of Human P-Glycoprotein Permits ATP Hydrolysis and Drug Transport, *Biochemistry*, **37**, 13660–13673.
- [86] **Loo, T. and Clarke, D.**, 1994. Reconstitution of drug-stimulated ATPase activity following co-expression of each half of human P-glycoprotein as separate polypeptides., *Journal of Biological Chemistry*, **269**, 7750.

- [87] **Ramachandra, M., Ambudkar, S.V. and Christine, D.C.**, 1998. Human P-glycoprotein exhibits reduced affinity for substrates during a catalytic transition state, *Biochemistry*, **37**, 5010–5019.
- [88] **Lam, F., Liu, R., Lu, P., Shapiro, A., Renoir, J., Sharom, F. and Reiner, P.**, 2001. beta-Amyloid efflux mediated by p-glycoprotein, *Journal of Neurochemistry*, **76**, 1121–112.
- [89] **Gatlik-Landwojtowicz, E., nismaa, P. and Seelig, A.**, 2006. Quantification and Characterization of P-Glycoprotein Substrate Interactions, *Biochemistry*, **45**, 3020–3032.
- [90] **Loe, D. and Sharom, F.**, 1994. Interaction of multidrug-resistant Chinese hamster ovary cells with the peptide ionophore gramicidin D, *Biochimica et Biophysica Acta (BBA)-Biomembranes*, **1190**, 72–84.
- [91] **Sharom, F., DiDiodato, G., Yu, X. and Ashbourne, K.**, 1995. Interaction of the P-glycoprotein multidrug transporter with peptides and ionophores, *Journal of Biological Chemistry*, **270**, 10334.
- [92] **Sharom, F., Yu, X., DiDiodato, G. and Chu, J.**, 1996. Synthetic hydrophobic peptides are substrates for P-glycoprotein and stimulate drug transport., *Biochemical Journal*, **320**, 421.
- [93] **Lugo, M. and Sharom, F.**, 2005. Interaction of LDS-751 and Rhodamine 123 with P-Glycoprotein: Evidence for Simultaneous Binding of Both Drugs, *Biochemistry*, **44**, 14020–14029.
- [94] **Loo, T. and Clarke, D.**, 1994. Functional consequences of glycine mutations in the predicted cytoplasmic loops of P-glycoprotein., *Journal of Biological Chemistry*, **269**, 7243.
- [95] **Seelig, A.**, 1998. A general pattern for substrate recognition by P-glycoprotein, *European Journal of Biochemistry*, **251**, 252 – 261.
- [96] **Seelig, A.**, 1998. How does P-glycoprotein recognize its substrates? , *International journal of clinical pharmacology and therapeutics*, **36**, 50–54.
- [97] **Ekins, S., Kim, R., Leake, B., Dantzig, A., Schuetz, E., Lan, L., Yasuda, K., Shepard, R., Winter, M. and Schuetz, J.**, 2002. Three-dimensional quantitative structure-activity relationships of inhibitors of P-glycoprotein, *Molecular pharmacology*, **61**, 964.
- [98] **Ekins, S., Kim, R., Leake, B., Dantzig, A., Schuetz, E., Lan, L., Yasuda, K., Shepard, R., Winter, M. and Schuetz, J.**, 2002. Application of three-dimensional quantitative structure-activity relationships of P-glycoprotein inhibitors and substrates, *Molecular pharmacology*, **61**, 974.
- [99] **Pajeva, I. and Wiese, M.**, 2002. Pharmacophore model of drugs involved in P-glycoprotein multidrug resistance: explanation of structural variety (hypothesis), *J. Med. Chem.*, **45**, 5671–5686.
- [100] **Cianchetta, G., Singleton, R., Zhang, M., Wildgoose, M., Giesing, D., Fravolini, A., Cruciani, G. and Vaz, R.**, 2005. A pharmacophore hypothesis for P-glycoprotein substrate recognition using GRIND-based 3D-QSAR, *J. Med. Chem.*, **48**, 2927–2935.

- [101] **Liu, R., Siemiarczuk, A. and Sharom, F.**, 2000. Intrinsic Fluorescence of the P-glycoprotein Multidrug Transporter: Sensitivity of Tryptophan Residues to Binding of Drugs and Nucleotides, *Biochemistry*, **39**, 14927–14938.
- [102] **Pawagi, A., Wang, J., Silverman, M., Reithmeier, R. and Deber, C.**, 1994. Transmembrane Aromatic Amino Acid Distribution in P-glycoprotein: A Functional Role in Broad Substrate Specificity, *Journal of molecular biology*, **235**, 554–564.
- [103] **Shapiro, A. and Ling, V.**, 1997. Positively cooperative sites for drug transport by P-glycoprotein with distinct drug specificities, *European Journal of Biochemistry*, **250**, 130–137.
- [104] **Loo, T., Bartlett, M. and Clarke, D.**, 2004. The Drug-Binding Pocket of the Human Multidrug Resistance P-Glycoprotein Is Accessible to the Aqueous Medium, *Biochemistry*, **43**, 12081–12089.
- [105] **Loo, T. and Clarke, D.**, 2005. Do drug substrates enter the common drug-binding pocket of P-glycoprotein through, *Biochemical and biophysical research communications*, **329**, 419–422.
- [106] **Garrigues, A., Loiseau, N., Delaforge, M., Ferte, J., Garrigos, M., Andre, F. and Orłowski, S.**, 2002. Characterization of two pharmacophores on the multidrug transporter P-glycoprotein, *Molecular pharmacology*, **62**, 1288.
- [107] **Globisch, C., Pajeva, I. and Wiese, M.**, 2008. Identification of putative binding sites of P-glycoprotein based on its homology model, *ChemMedChem*, **3**, 280–295.
- [108] **Chen, J., Lu, G., Lin, J., Davidson, A. and Quijcho, F.**, 2003. A tweezers-like motion of the ATP-binding cassette dimer in an ABC transport cycle, *Molecular cell*, **12**, 651–661.
- [109] **Oldham, M.L., Khare, D., Quijcho, F.A., Davidson, A.L. and Chen, J.**, 2007. Crystal structure of a catalytic intermediate of the maltose transporter, *Nature*, **450**, 515–522.
- [110] **Lee, J., Urbatsch, I., Senior, A. and Wilkens, S.**, 2008. Nucleotide-induced structural changes in P-glycoprotein observed by electron microscopy, *Journal of Biological Chemistry*, **283**, 5769.
- [111] **Loo, T.W., Bartlett, M.C. and Clarke, D.M.**, 2002. The LSGGQ motif in each nucleotide-binding domain of human P-glycoprotein is adjacent to the opposing walker A sequence, *The Journal Of Biological Chemistry*, **277**, 41303–41306.
- [112] **Smith, P., Karpowich, N., Millen, L., Moody, J., Rosen, J., Thomas, P. and Hunt, J.**, 2002. ATP binding to the motor domain from an ABC transporter drives formation of a nucleotide sandwich dimer, *Molecular cell*, **10**, 139–149.
- [113] **Hanekop, N., Zaitseva, J., Jenewein, S., Holland, I. and Schmitt, L.**, 2006. Molecular insights into the mechanism of ATP-hydrolysis by the NBD of the ABC-transporter HlyB, *FEBS letters*, **580**, 1036–1041.

- [114] **Tomblin, G., Bartholomew, L., Urbatsch, I. and Senior, A.**, 2004. Combined mutation of catalytic glutamate residues in the two nucleotide binding domains of P-glycoprotein generates a conformation that binds ATP and ADP tightly, *Journal of Biological Chemistry*, **279**, 31212.
- [115] **Tomblin, G., Muharemagić, A., White, L. and Senior, A.**, 2005. Involvement of the occluded nucleotide conformation of P-glycoprotein in the catalytic pathway, *Biochemistry*, **44**, 12879.
- [116] **Urbatsch, I., Gimi, K., Wilke-Mounts, S. and Senior, A.**, 2000. Investigation of the Role of Glutamine-471 and Glutamine-1114 in the Two Catalytic Sites of P-Glycoprotein, *Biochemistry*, **39**, 11921–11927.
- [117] **Zaitseva, J., Jenewein, S., Jumpertz, T., Holland, I. and Schmitt, L.**, 2005. H662 is the linchpin of ATP hydrolysis in the nucleotide-binding domain of the ABC transporter HlyB, *The EMBO Journal*, **24**, 1901–1910.
- [118] **Liu, R. and Sharom, F.**, 1996. Site-Directed Fluorescence Labeling of P-Glycoprotein on Cysteine Residues in the Nucleotide Binding Domains, *Biochemistry*, **35**, 11865–11873.
- [119] **Liu, R. and Sharom, F.**, 1997. Fluorescence Studies on the Nucleotide Binding Domains of the P-Glycoprotein Multidrug Transporter, *Biochemistry*, **36**, 2836–2843.
- [120] **Sauna, Z.E., Kim, I.W., Nandigama, K., Kopp, S., Chiba, P. and Ambudkar, S.V.**, 2007. Catalytic Cycle of ATP Hydrolysis by P-Glycoprotein: Evidence for Formation of the EAS Reaction Intermediate with ATP- γ -S, a Nonhydrolyzable Analogue of ATP, *Biochemistry*, **46**, 13787–13799.
- [121] **Al-Shawi, M., Polar, M., Omote, H. and Figler, R.**, 2003. Transition state analysis of the coupling of drug transport to ATP hydrolysis by P-glycoprotein, *Journal of Biological Chemistry*, **278**, 52629–52640.
- [122] **Senior, A., Al-Shawi, M. and Urbatsch, I.**, 1995. The catalytic cycle of P-glycoprotein, *FEBS letters*, **377**, 285–289.
- [123] **Loo, T. and Clarke, D.**, 1995. Covalent modification of human P-glycoprotein mutants containing a single cysteine in either nucleotide-binding fold abolishes drug-stimulated ATPase activity, *Journal of Biological Chemistry*, **270**, 22957.
- [124] **Delannoy, S., Urbatsch, I., Tomblin, G., Senior, A. and Vogel, P.**, 2005. Nucleotide Binding to the Multidrug Resistance P-Glycoprotein as Studied by ESR Spectroscopy, *Biochemistry*, **44**, 14010–14019.
- [125] **Qu, Q., Russell, P. and Sharom, F.**, 2003. Stoichiometry and Affinity of Nucleotide Binding to P-Glycoprotein during the Catalytic Cycle, *Biochemistry*, **42**, 1170–1177.
- [126] **Sauna, Z. and Ambudkar, S.**, 2000. Evidence for a requirement for ATP hydrolysis at two distinct steps during a single turnover of the catalytic cycle of human P-glycoprotein, *Proceedings of the National Academy of Sciences of the United States of America*, **97**, 2515.

- [127] **Sauna, Z. and Ambudkar, S.**, 2001. Characterization of the catalytic cycle of ATP hydrolysis by human P-glycoprotein, *Journal of Biological Chemistry*, **276**, 11653.
- [128] **Tomblin, G. and Senior, A.**, 2005. The occluded nucleotide conformation of p-glycoprotein, *Journal of bioenergetics and biomembranes*, **37**, 497–500.
- [129] **Romsicki, Y. and Sharom, F.**, 1999. The Membrane Lipid Environment Modulates Drug Interactions with the P-Glycoprotein Multidrug Transporter, *Biochemistry*, **38**, 6887–6896.
- [130] **Seelig, A. and LI, B.**, 2000. Substrate recognition by P-glycoprotein and the multidrug resistance-associated protein MRP1: a comparison: Special issue: Clinical Pharmacology of P-glycoprotein and related transporters, *International journal of clinical pharmacology and therapeutics*, **38**, 111–121.
- [131] **Higgins, C. and Gottesman, M.**, 1992. Is the multidrug transporter a flippase? , *Trends in biochemical sciences*, **17**, 18.
- [132] **Sharom, F.**, 2003. Probing of conformational changes, catalytic cycle and ABC transporter function, ABC Proteins: From Bacteria to Man, Academic Press, pp. 107–133.
- [133] **Loo, T. and Clarke, D.**, 1997. Drug-stimulated ATPase activity of human P-glycoprotein requires movement between transmembrane segments 6 and 12, *Journal of Biological Chemistry*, **272**, 20986.
- [134] **Sharom, F.**, 2006. Shedding light on drug transport: structure and function of the P-glycoprotein multidrug transporter (ABCB1), *Biochemistry and Cell Biology*, **84**, 979–992.
- [135] **Litman, T., Zeuthen, T., Skovsgaard, T. and Stein, W.**, 1997. Structure-activity relationships of P-glycoprotein interacting drugs: kinetic characterization of their effects on ATPase activity, *Biochimica et Biophysica Acta (BBA)-Molecular Basis of Disease*, **1361**, 159–168.
- [136] **Loo, T., Bartlett, M. and Clarke, D.**, 2003. Drug binding in human P-glycoprotein causes conformational changes in both nucleotide-binding domains, *Journal of Biological Chemistry*, **278**, 1575.
- [137] **Higgins, C. and Linton, K.**, 2004. The ATP switch model for ABC transporters, *Nature structural and molecular biology*, **11**, 918–926.
- [138] **Sankaran, B., Bhagat, S. and Senior, A.**, 1997. Inhibition of P-glycoprotein ATPase activity by procedures involving trapping of nucleotide in catalytic sites, *Archives of biochemistry and biophysics*, **341**, 160–169.
- [139] **Omote, H., Figler, R., Polar, M. and Al-Shawi, M.**, 2004. Improved Energy Coupling of Human P-glycoprotein by the Glycine 185 to Valine Mutation, *Biochemistry*, **43**, 3917–3928.
- [140] **Urbatsch, I., Sankaran, B., Weber, J. and Senior, A.**, 1995. P-glycoprotein is stably inhibited by vanadate-induced trapping of nucleotide at a single catalytic site, *Journal of Biological Chemistry*, **270**, 19383.

- [141] **Qu, Q., Chu, J. and Sharom, F.**, 2003. Transition State P-glycoprotein Binds Drugs and Modulators with Unchanged Affinity, Suggesting a Concerted Transport Mechanism, *Biochemistry*, **42**, 1345–1353.
- [142] **Loo, T. and Clarke, D.**, 2002. Vanadate trapping of nucleotide at the ATP-binding sites of human multidrug resistance P-glycoprotein exposes different residues to the drug-binding site, *Proceedings of the National Academy of Sciences of the United States of America*, **99**, 3511.
- [143] **Mather, R.**, 2008. Characterizing The Substrate Binding Pocket Of The P-Glycoprotein Multi-Drug Efflux Pump, Master's thesis, The University of Guelph.
- [144] **Loo, T., Bartlett, M. and Clarke, D.**, 2003. Permanent activation of the human P-glycoprotein by covalent modification of a residue in the drug-binding site, *Journal of Biological Chemistry*, **278**, 20449.
- [145] **Krupka, R.**, 1999. Uncoupled active transport mechanisms accounting for low selectivity in multidrug carriers: P-glycoprotein and SMR antiporters, *Journal of Membrane Biology*, **172**, 129–143.
- [146] **Al-Shawi, M. and Omote, H.**, 2005. The remarkable transport mechanism of P-glycoprotein: a multidrug transporter, *Journal of bioenergetics and biomembranes*, **37**, 489–496.
- [147] **Kureishi, Y., Luo, Z., Shiojima, I., Bialik, A., Fulton, D., Lefer, D., Sessa, W. and Walsh, K.**, 2000. The HMG-CoA reductase inhibitor simvastatin activates the protein kinase Akt and promotes angiogenesis in normocholesterolemic animals., *Nature Medicine*, **6**, 1004–1010.
- [148] **Mundy, G., Garrett, R., Harris, S., Chan, J., Chen, D., Rossini, G., Boyce, B., Zhao, M. and Gutierrez, G.**, 1999. Stimulation of bone formation *in vitro* and in rodents by statins, *Science*, **286**, 1946.
- [149] **Davignon, J. and Laaksonen, R.**, 1999. Low-density lipoprotein-independent effects of statins, *Current Opinion in Lipidology*, **10**, 543.
- [150] **Miida, T., Hirayama, S. and Nakamura, Y.**, 2004. Cholesterol-independent effects of statins and new therapeutic targets: ischemic stroke and dementia, *Journal of atherosclerosis and thrombosis*, **11**, 253–264.
- [151] **Corsini, A., Maggi, F. and Catapano, A.**, 1995. Pharmacology of competitive inhibitors of HMG-CoA reductase., *Pharmacological research: the official journal of the Italian Pharmacological Society*, **31**, 9.
- [152] **Endo, A., Kuroda, M. and Tanzawa, K.**, 1976. Competitive inhibition of 3-hydroxy-3-methylglutaryl coenzyme A reductase by ML-236A and ML-23613, fungal metabolites having hypocholesterolemic activity, *FEBS Lett*, **72**, 323–326.
- [153] **Bischoff, K. and Rodwell, V.**, 1992. Biosynthesis and characterization of (S)- and (R)-3-hydroxy-3-methylglutaryl coenzyme A, *Biochemical medicine and metabolic biology*, **48**, 149–158.

- [154] **Graham, D., Staffa, J., Shatin, D., Andrade, S., Schech, S., La Grenade, L., Gurwitz, J., Chan, K., Goodman, M. and Platt, R.**, 2004. Incidence of hospitalized rhabdomyolysis in patients treated with lipid-lowering drugs, *Jama*, **292**, 2585.
- [155] **Backman, J., Kyrklund, C., Neuvonen, M. and Neuvonen, P.**, 2002. Gemfibrozil greatly increases plasma concentrations of cerivastatin&ast, *Clinical Pharmacology and Therapeutics*, **72**, 685–691.
- [156] **Wang, E., Casciano, C., Clement, R. and Johnson, W.**, 2001. HMG-CoA reductase inhibitors (statins) characterized as direct inhibitors of P-glycoprotein, *Pharmaceutical research*, **18**, 800–806.
- [157] **Bogman, K., Peyer, A., Torok, M., Kusters, E. and Drewe, J.**, 2001. HMG-CoA reductase inhibitors and P-glycoprotein modulation, *British journal of pharmacology*, **132**, 1183.
- [158] **Wu, X., Whitfield, L. and Stewart, B.**, 2000. Atorvastatin transport in the Caco-2 cell model: contributions of P-glycoprotein and the proton-monocarboxylic acid co-transporter, *Pharmaceutical research*, **17**, 209–215.
- [159] **Hochman, J., Pudvah, N., Qiu, J., Yamazaki, M., Tang, C., Lin, J. and Prueksaritanont, T.**, 2004. Interactions of human P-glycoprotein with simvastatin, simvastatin acid, and atorvastatin, *Pharmaceutical research*, **21**, 1686–1691.
- [160] **Boyd, R., Stern, R., Stewart, B., Wu, X., Reyner, E., Zegarac, E., Randinitis, E. and Whitfield, L.**, 2000. Atorvastatin coadministration may increase digoxin concentrations by inhibition of intestinal P-glycoprotein-mediated secretion, *The Journal of Clinical Pharmacology*, **40**, 91.
- [161] **Sakaeda, T., Fujino, H., Komoto, C., Kakumoto, M., Jin, J., Iwaki, K., Nishiguchi, K., Nakamura, T., Okamura, N. and Okumura, K.**, 2006. Effects of acid and lactone forms of eight HMG-CoA reductase inhibitors on CYP-mediated metabolism and MDR1-mediated transport, *Pharmaceutical research*, **23**, 506–512.
- [162] **Sakaeda, T., Takara, K., Kakumoto, M., Ohmoto, N., Nakamura, T., Iwaki, K., Tanigawara, Y. and Okumura, K.**, 2002. Simvastatin and lovastatin, but not pravastatin, interact with MDR1., *The Journal of pharmacy and pharmacology*, **54**, 419.
- [163] **Christians, U., Schmitz, V. and Haschke, M.**, 2005. Functional interactions between P-glycoprotein and CYP3A in drug metabolism, *Expert Opin. Drug Metab. Toxicol.*, **1**, 641–654.
- [164] **Holtzman, C., Wiggins, B. and Spinler, S.**, 2006. Role of P-glycoprotein in statin drug interactions, *Pharmacotherapy*, **26**, 1601–1607.
- [165] **Kirn, R., Wandel, C., Leake, B., Cvetkovic, M., Fromm, M., Dempsey, P., Roden, M., Belas, F., Chaudhary, A. and Roden, D.**, 1999. Interrelationship between substrates and inhibitors of human CYP3A and P-glycoprotein, *Pharmaceutical research*, **16**, 408–414.

- [166] **Wacher, V., Wu, C. and Benet, L.**, 1995. Overlapping substrate specificities and tissue distribution of cytochrome P450 3A and P-glycoprotein: implications for drug delivery and activity in cancer chemotherapy, *Molecular Carcinogenesis*, **13**, 129–134.
- [167] **Williams, D. and Feely, J.**, 2002. Pharmacokinetic-pharmacodynamic drug interactions with HMG-CoA reductase inhibitors, *Clinical pharmacokinetics*, **41**, 343–370.
- [168] **Corsini, A., Bellosta, S., Baetta, R., Fumagalli, R., Paoletti, R. and Bernini, F.**, 1999. New insights into the pharmacodynamic and pharmacokinetic properties of statins, *Pharmacology and therapeutics*, **84**, 413–428.
- [169] **McCormick, A., McKillop, D., Butters, C., Miles, G., Baba, T., Touchi, A. and Yamaguchi, Y.**, 2000. ZD4522-an HMG-CoA reductase inhibitor free of metabolically mediated drug interactions: metabolic studies in human *in vitro* systems, *J Clin Pharmacol*, **40**, 1055.
- [170] **Lindahl, E.**, 2008. Molecular Dynamics Simulations, Molecular Modeling of Proteins, Humana Press, pp. 3–23.
- [171] **Alder, B. and Wainwright, T.**, 1957. Phase transition for a hard sphere system, *The Journal of Chemical Physics*, **27**, 1208.
- [172] **Rahman, A. and Stillinger, F.**, 1971. Molecular dynamics study of liquid water, *The Journal of Chemical Physics*, **55**, 3336.
- [173] **McCammon, J., Gelin, B. and Karplus, M.**, 1977. Dynamics of folded proteins, *Nature*, **267**, 585.
- [174] **Allen, M. and Tildesley, D.**, 1989. Computer Simulation of Liquids., Clarendon Press.
- [175] **Frenkel, D. and Smit, B.**, 2001. Understanding Molecular Simulation, Academic Press.
- [176] **Kaminski, G., Friesner, R., Tirado-Rives, J. and Jorgensen, W.**, 2001. Evaluation and reparametrization of the OPLS-AA force field for proteins via comparison with accurate quantum chemical calculations on peptides, *J. Phys. Chem*, **105**, 6474–6487.
- [177] **MacKerell, A., Brooks, B., Brooks III, C., Nilsson, L., Roux, B., Won, Y. and Karplus, M.**, 1998. CHARMM: the energy function and its parameterization with an overview of the program, *The encyclopedia of computational chemistry*, **1**, 271–277.
- [178] **Oostenbrink, C., Villa, A., Mark, A. and van Gunsteren, W.**, 2004. A biomolecular force field based on the free enthalpy of hydration and solvation: the GROMOS force-field parameter sets 53A5 and 53A6, *Journal of Computational Chemistry*, **25**, 1656–1676.
- [179] **Wang, J., Cieplak, P. and Kollman, P.**, 2000. How well does a restrained electrostatic potential (RESP) model perform in calculating conformational energies of organic and biological molecules? , *J. Comput. Chem*, **21**, 1049–1074.

- [180] **Leach, A.**, 2001. *Molecular modelling: principles and applications*, Prentice Hall, Harlow, UK.
- [181] **Essmann, U., Perera, L., Berkowitz, M., Darden, T., Lee, H. and Pedersen, L.**, 1995. A smooth particle mesh Ewald method, *Journal of Chemical Physics*, **103**, 8577–8593.
- [182] **Ryckaert, J., Ciccotti, G. and Berendsen, H.**, 1977. Numerical integration of the cartesian equations of motion of a system with constraints: molecular dynamics of n-alkanes, *J. Comp. Phys*, **23**, 327–341.
- [183] **Hess, B., Bekker, H., Berendsen, H. and Fraaije, J.**, 1997. 3 LINCS: a linear constraint solver for molecular simulations, *J Comput Chem*, **18**, 1463–1472.
- [184] **Wang, W., Donini, O., Reyes, C. and Kollman, P.**, 2001. Biomolecular simulations: recent developments in force fields, simulations of enzyme catalysis, protein-ligand, protein-protein, and protein-nucleic acid noncovalent interactions, *Annu. Rev. Biophys. Biomol. Struct*, **30**, 211–243.
- [185] **Mackerell, A.**, 2004. Empirical force fields for biological macromolecules: overview and issues, *Journal of computational chemistry*, **25**, 1584–1604.
- [186] **Cornell, W., Cieplak, P., Bayly, C., Gould, I., Merz, K., Ferguson, D., Spellmeyer, D., Fox, T., Caldwell, J. and Kollman, P.**, 1995. A new force field for molecular mechanical simulation of nucleic acids and proteins, *J. Am. Chem. Soc*, **117**, 5179–5197.
- [187] **Scott, W., Hunenberger, P., Tironi, I., Mark, A., Billeter, S., Fennen, J., Torda, A., Huber, T., Kruger, P. and van Gunsteren, W.**, 1999. The GROMOS biomolecular simulation program package, *J. Phys. Chem. A*, **103**, 3596–3607.
- [188] **Jorgensen, W., Chandrasekhar, J., Madura, J., Impey, R. and Klein, M.**, 1983. Comparison of simple potential functions for simulating liquid water, *The Journal of Chemical Physics*, **79**, 926.
- [189] **Berman, H., Battistuz, T., Bhat, T., Bluhm, W., Bourne, P., Burkhardt, K., Feng, Z., Gilliland, G., Iype, L. and Jain, S.**, 2002. The protein data bank, *Acta Crystallographica Section D: Biological Crystallography*, **58**, 899–907.
- [190] **Kukol, A.**, 2006. Lipid Models for United-Atom Molecular Dynamics Simulations of Proteins, *J. Chem. Theory Comput.*, **5 (3)**, 615–626.
- [191] **Kandt, C., Xu, Z. and Tieleman, D.**, 2006. Opening and Closing Motions in the Periplasmic Vitamin B12 Binding Protein BtuF, *Biochemistry*, **45**, 13284–13292.
- [192] **Wolf, M., Hoefling, M., Aponte-Santamaria, C., Grubmuller, H. and Groenhof, G.**, 2010. g_membed: Efficient insertion of a membrane protein into an equilibrated lipid bilayer with minimal perturbation, *Journal of Computational Chemistry*.

- [193] **Seeliger, D. and de Groot, B.**, 2010. Ligand docking and binding site analysis with PyMOL and Autodock/Vina, *Journal of computer-aided molecular design*, **24**, 417–422.
- [194] **Trott, O. and Olson, A.**, 2010. AutoDock Vina: improving the speed and accuracy of docking with a new scoring function, efficient optimization, and multithreading, *Journal of Computational Chemistry*, **31**, 455–461.
- [195] **Berendsen, H., Postma, J., van Gunsteren, W., DiNola, A. and Haak, J.**, 1984. Molecular dynamics with coupling to an external bath, *The Journal of Chemical Physics*, **81**, 3684.
- [196] **Nose, S.**, 1984. A molecular dynamics method for simulations in the canonical ensemble, *Molecular Physics*, **52**, 255–268.
- [197] **Hoover, W.**, 1985. Canonical dynamics: Equilibrium phase-space distributions, *Physical Review A*, **31**, 1695–1697.
- [198] **Parrinello, M. and Rahman, A.**, 1981. Polymorphic transitions in single crystals: A new molecular dynamics method, *Journal of Applied Physics*, **52**, 7182.
- [199] **Darden, T., York, D. and Pedersen, L.**, 1993. Particle mesh Ewald: An N.log(N) method for Ewald sums in large systems, *The Journal of Chemical Physics*, **98**, 10089.
- [200] **Hermans, J., Berendsen, H., van Gunsteren, W. and Postma, J.**, 1984. A consistent empirical potential for water-protein interactions, *Biopolymers*, **23**.
- [201] **Berendsen, H., Van der Spoel, D. and Van Drunen, R.**, 1995. GROMACS: a message-passing parallel molecular dynamics implementation, *Computer Physics Communications*, **91**, 43–56.
- [202] **Lindahl, E., Hess, B. and van der Spoel, D.**, 2001. GROMACS 3.0: a package for molecular simulation and trajectory analysis, *Journal of Molecular Modeling*, **7**, 306–317.
- [203] **Van Der Spoel, D., Lindahl, E., Hess, B., Groenhof, G., Mark, A. and Berendsen, H.**, 2005. GROMACS: fast, flexible, and free, *Journal of Computational Chemistry*, **26**, 1701–1718.
- [204] **Medek, P., Benevs, P. and Sochor, J.**, 2007. Computation of tunnels in protein molecules using Delaunay triangulation, *Journal of WSCG*, **15**, 107–114.
- [205] **Humphrey, W., Dalke, A. and Schulten, K.**, 1996. VMD: visual molecular dynamics, *Journal of Molecular Graphics*, **14**, 33–38.
- [206] **DeLano, W.**, 2002.
- [207] **Amadei, A., Linssen, A. and Berendsen, H.**, 1993. Essential dynamics of proteins, *Proteins: Structure, Function, and Genetics*, **17**.
- [208] **Kitao, A., Hirata, F. and Go, N.**, 1991. The effects of solvent on the conformation and the collective motions of protein: normal mode analysis and molecular dynamics simulations of melittin in water and in vacuum, *Chemical physics*, **158**, 447–472.

- [209] **Garcia, A.**, 1992. Large-amplitude nonlinear motions in proteins, *Physical review letters*, **68**, 2696–2699.
- [210] **Ivetac, A., Campbell, J. and Sansom, M.**, 2007. Dynamics and Function in a Bacterial ABC Transporter: Simulation Studies of the BtuCDF System and Its Components, *Biochemistry*, **46**, 2767–2778.
- [211] **Filippov, A., Oradd, G. and Lindblom, G.**, 2003. Influence of Cholesterol and Water Content on Phospholipid Lateral Diffusion in Bilayers, *Langmuir*, **19**, 6397–6400.
- [212] **Douliez, J., Leonard, A. and Dufourc, E.**, 1995. Restatement of order parameters in biomembranes: calculation of CC bond order parameters from CD quadrupolar splittings, *Biophysical journal*, **68**, 1727–1739.
- [213] **Hildebrand, P., Gunther, S., Goede, A., Forrest, L., Frommel, C. and Preissner, R.**, 2008. Hydrogen-bonding and packing features of membrane proteins: functional implications, *Biophysical journal*, **94**, 1945–1953.
- [214] **Becker, J.P., Van Bambeke, F., Tulkens, P.M. and Provost, M.**, 2010. Dynamics and Structural Changes Induced by ATP Binding in SAV1866, a Bacterial ABC Exporter, *The Journal of Physical Chemistry B*, **0**.
- [215] **Aittoniemi, J., de Wet, H., Ashcroft, F. and Sansom, M.**, 2010. Asymmetric Switching in a Homodimeric ABC Transporter: A Simulation Study, *PLoS Comput Biol*, **6**, e1000762.

CURRICULUM VITAE



Candidate's full name: Deniz KARASU

Place and date of birth: 02.12.1978

Permanent Address: Selimiye quarter, Bestekar Avni Anıl St. Hamle Apt.
No:15/12 Üsküdar / İSTANBUL

Universities and Colleges attended:

- **M.Sc.** (2008-2010) Istanbul Technical University, Molecular Biology and Genetic Department
- **B.Eng.** (1998-2002) Istanbul University, Industrial Engineering